BIOCHEMICAL CHARACTERISATION OF ABHD14A: AN ORPHAN PROTEIN

विद्या वाचस्पति की
उपाधि की अपेक्षाओं की आंशिक पूर्ति में प्रस्तुत शोध प्रबंध

A thesis submitted in partial fulfillment of the requirements of the degree of

Doctor of Philosophy

द्वारा / By

सोनाली गुप्ता/ Sonali Gupta

पंजीकरण सं. / Registration No.: 20192005

शोध प्रबंध पर्यवेक्षक / Thesis Supervisor: Dr. Siddhesh S. Kamat

भारतीय विज्ञान शिक्षा एवं अनुसंधान संस्थान पुणे

INDIAN INSTITUTE OF SCIENCE EDUCATION AND RESEARCH PUNE

2026

DEDICATION

I dedicate this work to my mumma and pitashree

MRS. MANJU GUPTA and MR. DEVENDER KUMAR GUPTA

and to bhaiya

MR. NISHANT GUPTA

CERTIFICATE

Certified that the work incorporated in the thesis entitled "Biochemical Characterisation of ABHD14A: an orphan protein" submitted by Sonali Gupta was carried out by the candidate, under my supervision. The work presented here or any part of it has not been included in any other thesis submitted previously for the award of any degree or diploma from any other University or institution.

डॉ. सिध्देश कामत/Dr. Siddhesh Kamat
प्राध्यापक/ Professor
जीवशास्त्र विभाग / Biology Department
भारतीय विज्ञान शिक्षा एवं अनुसंधान संस्थान
Indian Institute of Science Education & Research
पुणे / Pune- 411 008, भारत / India

Supervisor

Date: 05-01-2026

DECLARATION

Name of Student: Sonali Gupta

Reg. No.: 20192005

Thesis Supervisor(s): Dr. Siddhesh S. Kamat

Department: Biology

Date of joining program: 01-08-2019

Date of Pre-Synopsis Seminar: 12-12-2025

Title of Thesis: Biochemical characterisation of ABHD14A: an orphan protein

I declare that this written submission represents my idea in my own words and where others' ideas have been included; I have adequately cited and referenced the original sources. I declare that I have acknowledged collaborative work and discussions wherever such work has been included. I also declare that I have adhered to all principles of academic honesty and integrity and have not misrepresented or fabricated or falsified any idea/data/fact/source in my submission. I understand that violation of the above will be cause for disciplinary action by the Institute and can also evoke penal action from the sources which have thus not been properly cited or from whom proper permission has not been taken when needed.

The work reported in this thesis is the original work done by me under the guidance of Dr. Siddhesh S. Kamat.
Date: 05-01-2026

Signature of the student: 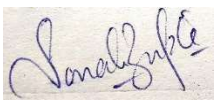

ACKNOWLEDGEMENTS

I would like to express my devout gratitude to everyone who has contributed to the completion of this thesis. First and foremost, I would like to thank my supervisor, Dr. Siddhesh S. Kamat for giving me the opportunity to work on this project and for his constant guidance, support and understanding throughout the years. I am especially thankful to him for giving me the liberty to explore new directions in this field with respect to the experiments that I performed. I am also thankful to members of my Research Advisory Committee, Dr. Amrita Hazra and Dr. Krishanpal Karmodiya for their time and insights along with feedback for the project. I would also like to express my sincere gratitude to the fellow professors and the non-teaching and technical staff of the Department of Biology for the timely and efficient support with technical and administration related work. I would specifically like to thank the Mass Spectrometry facility at IISER Pune, especially Mr. Shekh Saddam Husen Shekh Hamja (Technical Assistant) for the timely and efficient support. I would also like to thank the Microscopy facility and National Facility for Gene Function in Health and Disease for their collaborative efforts in the project. I would also like to thank my fellow graduate students and professors in the department for the gracious and kind help with chemicals and inputs, whenever needed. Overall, I would like to thank IISER Pune for the educational and research facilities.
I would like to thank the Prime Minister's Research Fellowship for funding me during the course of this project and the IISER Pune IDeaS Scholarship for the tution fee waiver during my master's education. I would also like to thank Fergusson college for giving me the opportunity to teach there.

I would also like to thank all the past and present members of Kamat Lab for the extremely relaxed and jovial environment in the lab, and for all the activities outside of lab. I would like to thank Dr. Abinaya Rajendran and Dr. Kaveri Vaidya for their enormous support and inspiring mentorship. I would especially like to mention all the rotation students who contributed with their help to this project.

I would like to express my deepest regards to my teachers in my bachelor's education for giving us the best understanding of biochemistry and its concepts and for the being a constant

support till date: Dr. K. Nirmala, Dr. Sunita Joshi, Dr. Padamshree Mudgal, Dr. Sarita Nanda, Dr. Anita Mangla, Dr. Neeru Dhamija and Dr. Leena Vij.

I would like to express my deepest thanks to the 22 women from my bachelors who I will always be inspired by and continue to cherish for my life. These women have not only set examples for me in terms of grit and excellence, but they also regularly remind me of kindness and support that the world has to offer. I knew no joy if it were not for the time spent with them.

I would also especially like to acknowledge the Integrated PhD batch of 2019 (Biology) for being the best set of individuals to start off this journey with. I am always overwhelmed by the amount of love and support that they have provided to me and continue to do. I could not have finished most of my experiments if it weren't for them all and their last-minute aid. I have only sought inspiration from all of them in terms of talent and hard work. They have been my family away from home. They will always be a very special part of this journey: Devatrisha Purkhayasta, Dhrubojyoti Patra, Mohit Mantri, Radhika Malaviya, Roopsali Banerjee, Sanhita Sarkar, Saswati Kar, Sayantan Banerjee, Sucharita Sen, Susobhan Das, Unnimaya.

I would also like to thank some special friends who have been instrumental in this journey and will be endeared for life: Kaveri Vaidya, Sivang Goswami, Archit Devarajan and Chaitanya Katkar. I would also want to dedicate this work to all of my friends who weren't here but supported me from afar: Mudit Srivastava, Soumya, Vaishnavi, Amisha, Abreeta, Ankita, Anshi, Shefali, Vranda, Bhawna, Akankshya and Manisha.

Finally, I would like to thank my parents, Mrs. Manju Gupta and Mr. Devender Kumar Gupta, and brother (Nishant Gupta) for being my biggest cheerleaders in every endeavour. They have been the constant support and encouragement that I needed during this time and its with their love and motivation that I could successfully finish this work. I am indebted to them for keeping faith in me for everything I do.

In the end, I would like to thank God for everything he has graced me with and for everything ahead.

TABLE OF CONTENTS

LIST OF FIGURES

LIST OF TABLES

ABSTRACT

Biochemical characterisation of ABHD14A: an orphan protein

The advent of genome sequencing technologies has revealed the presence of a myriad of proteins in the mammalian system, many of which are poorly characterised. The presence of these orphan proteins imply that our understanding of cell and tissue metabolism and its associated biochemical pathways is still dismal, underscoring the roles of these additional molecular players. Therefore, the functional annotation of these orphan proteins provides great avenues to understand their biochemistry and their physiological implications in health and disease. Enzymes of the serine hydrolase family are of particular interest in this regard, since members of this family metabolize a wide range of physiological substrates including peptides and proteins, lipids and small molecules, with a large fraction of these still unannotated. Alpha beta hydrolase domain containing protein 14A is one such uncharacterised enzyme. In our study, we sought characterisation with first identifying sequence determinants for the efficient annotation of the protein across organismic classes. We have established protocols for purifying this scarcely researched protein and used chemo proteomic methods to assay its biochemical activity, with emphasis on similar activity on induced expression in cultured cells. We also predict hydrolase activity using preferred substrates. To further investigate the roles of ABHD14A, we developed an antibody against the purified protein and characterised it using different experiments. Overall, using the novel standardised methods for assessing the activity of ABHD14A, we have tried to understand its role in mammalian biochemistry, by probing diverse aspects, including its subcellular localisation, spatiotemporal expression and metabolic changes upon induced expression.

CHAPTER 1

INTRODUCTION TO ABHD14A AND ITS PUTATIVE SIGNIFICANCE IN MAMMALIAN BIOCHEMISTRY

The advent of genome sequencing technologies has revealed the presence of many new and unknown sequences in prokaryotic as well as eukaryotic systems, with many databases curating information about the same. The Human Genome project in 2003 was a consequence of efforts by multiple scientists that gave us the concrete roadmap of the human genome for the first time[1]. The project was successful due to the advancements in sequencing and analytical techniques. The successive efforts to study the genome and its translational products by transcriptomics and proteomics revealed that humans code for more than 20,000 proteins. Excitingly, a multitude of such databases have revealed the presence of a vast repertoire of unrecognized and understudied proteins across organisms, pertaining to a major fraction of these sequences. The presence of these orphan proteins, which have also remained conserved across species, imply that our understanding of cell and tissue metabolism and its associated biochemical pathways is still dismal, underscoring the roles of these additional molecular players, especially in mammalian systems. This knowledge gap is further widened due to the extensive research bias towards the well-studied proteins that have proved instrumental in disease diagnostics, and therefore disguised the venture for the "unknowme" niche.

The unknowme database was curated by Sean Munro's group in the LMB's Cell Biology Division, which ranks proteins based on how little is known about them[2]. They started with a list of all ~20,000 human proteins and collected all the information that is available about their function, or the function of the closely related proteins from model organisms like mice, flies, or yeast. They then assigned each protein a "knownness" score depending on the quantity of available knowledge. To assess the value of the database, 260 genes in humans were selected for which there are comparable genes in fruit flies but almost nothing is known about their function. They used RNA interference to remove the corresponding proteins from fruit flies. They found that over a quarter are essential for flies to live. Further screens showed that a large fraction of the remaining proteins contribute to important functions including fertility, development, tissue growth, protein quality control, or stress resistance. This implies that we have been ignoring key molecular players

for decades and there is an imperative need to study these unannotated proteins, also encompassing disease physiology.

Therefore, the functional annotation of these orphan proteins poses a great challenge and opportunity for researchers in the postgenomic era, providing great avenues to understand their biochemistry and their physiological implications in health and disease.

Enzymes of the serine hydrolase family are of particular interest in this regard, since members of this family metabolize a wide range of physiological substrates including peptides and proteins, lipids and small molecules, through a conserved catalytic mechanism. This is the largest functional enzyme class in humans (nearly 1% of the proteome), with about 200 members, with diverse domains of activities such as esterases, thioesterases, lipases, proteases, dehalogenases, haloperoxidases, and epoxide hydrolases[3,4]. These diverse roles translate to their regulatory roles in various pathophysiological processes like neurotransmission, cancer, digestion, blood clotting, oxidative stress, immunity etc. Research on these proteins has also shifted the focus on the development of various inhibitors which have shown to act as therapeutics for multiple diseases. Prominent examples include the inhibitors of thrombin, acetylcholinesterase and dipeptidyl peptidase 4 that are used to treat clotting disorders, Alzheimer's disease-associated dementia and diabetes, respectively[5].

The first few studies on this class of enzymes emerged from a combination of crystallography, chemical labelling and mutational studies on chymotrypsin and trypsin[6]. Chymotrypsin, which was a fairly easy enzyme to purify due to a single subunit and active site, was crystallised and the amino acids were mapped on the structure. Chemical studies with diisopropyl fluorophosphate (DFP), revealed that it forms a covalent adduct with only one serine (Ser195) of the protein and blocking this serine led to complete loss of activity for the enzyme[7,8]. Similar inspections with other proteins revealed the same serine residue to be responsible for the activity of these enzymes[9,10]. Further colorimetric assays and structural studies also helped in deducing a mechanism of action for these enzymes[11,12]. The serine is residue present as part of a catalytic dyad or triad (Figure 1.1) in the active site with the following roles: Oγ atom of the serine acts as the nucleophile, the imidazole ring of the histidine, which serves as a general acid/base abstracts a proton from the serine OH group, and the carboxylate of an aspartic acid, which helps to orient the

imidazole ring by stabilising the positively charged histidine. In addition, an oxyanion hole provides electrophilic assistance to the nucleophilic attack by the serine Oγ on the carbonyl atom of the scissile bond. The hydrolysis reaction advances through the formation of an acyl-enzyme intermediate, with the activated serine Oɣ atom attacking an electron deficient bond in the substrate, followed by the release of the first product and the successive hydrolytic attack of a water molecule to release the free enzyme and the second product (Figure 1.2)[13]. Some well-studied serine hydrolases include: carboxylpeptidase, hormone sensitive lipase, fibroblast activation protein etc[3].

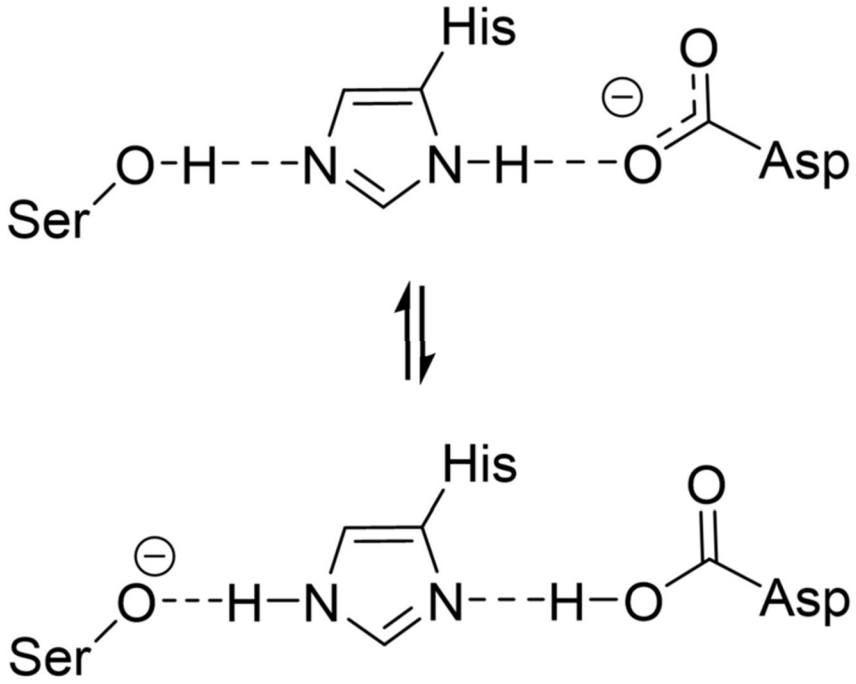

Figure-1.1: Charge relay system in a catalytic triad of serine hydrolases.[14]

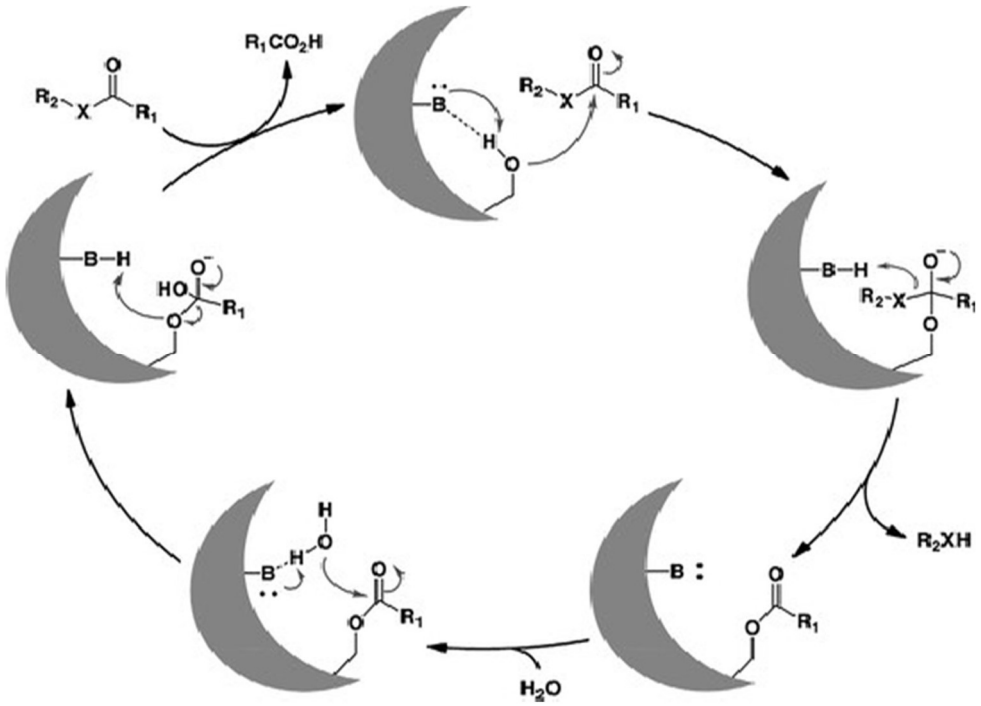

Figure 1.2: Conserved Catalytic Mechanism of the Metabolic Serine Hydrolase Family of Enzymes[13]

Serine hydrolases can be classified into two major categories: the peptidases or proteases and the metabolic serine hydrolases[3]. The former have been extensively studied and act majorly on peptide bonds, while the latter are described to hydrolyse ester, amide or thioester bonds in their in vivo substrates. The enzymology of many metabolic serine hydrolases is yet in a state of infancy but the study of various metabolic diseases and the advancement of metabolomic and proteomic techniques have revealed putative roles for these enzymes in the living system biochemistry.

Many proteins in the metabolic serine hydrolase family have adopted the conserved alpha/beta hydrolase fold in their structure. This fold was first identified by David et al.,1992 in an attempt to study convergent and divergent evolution of proteins[15]. They studied the structure of five enzymes, totally unrelated by their substrate specificities, source, and the chemistry of the reaction they catalyze. The enzymes were Acetylcholine esterase (Ach), from *Torpedo californica*, carboxypeptidase II (CPW) from wheat, dienelactone hydrolase (DLH) from *Pseudomonas sp.B13*, haloalkane dehalogenase (HAL) from *Xanthobacterautotrophicus* and lipase (GLP) from *Geotrichumcandidum*. A detailed comparative study of the five enzymes revealed that all of them had a common central fold, which they termed as the α/β hydrolase fold. The fold is

composed of eight beta strands sandwiched by alpha helices (Figure 1.3). Unlike a barrel, the beta-sheet is not continuous, and the topology can be described as 12435678, with the second beta-strand being antiparallel to the first, the rest others maintaining the orientation. The topology can better be described by the connecting loops, which serve the following order: +1, +2, -1x, +2x, $(+1x)_3$(Richardson, 1981), where x represents a crossover connection and the sole numeric value represents a hairpin loop. The number associated tells the connection with the next beta-strand, and (±) represents the ascent of the chain. The beta-strands are interspersed with six alpha-helices (canonical fold), named from A-F. The alpha/beta hydrolase domain also has a twist associated with it, such that the first and the last beta strands lie at an angle of 90 degrees from each other[16]. The packing of helices also varies throughout the fold structure, with helices A and F packing against the concave surface of the beta-sheet and B-E helices crate on the convex surface[16,17]. This canonical structure is marked by differences throughout the protein superfamily, with many proteins having added helices and beta strands at the C terminal, a few angular modifications, etc. But the characteristic feature of the fold, which imparts its catalytic activity of performing hydrolysis reactions, is the catalytic triad. The catalytic triad is present in the order of nucleophile-acid-histidine, with their topological location and order conserved throughout the fold parentage[18]. The superposition of tertiary structures of various proteins which contain this fold about the catalytic residues gives added conserved features in the domain, and this conserved identity of thousands of proteins places them under this large group of proteins despite the presence of other domains.

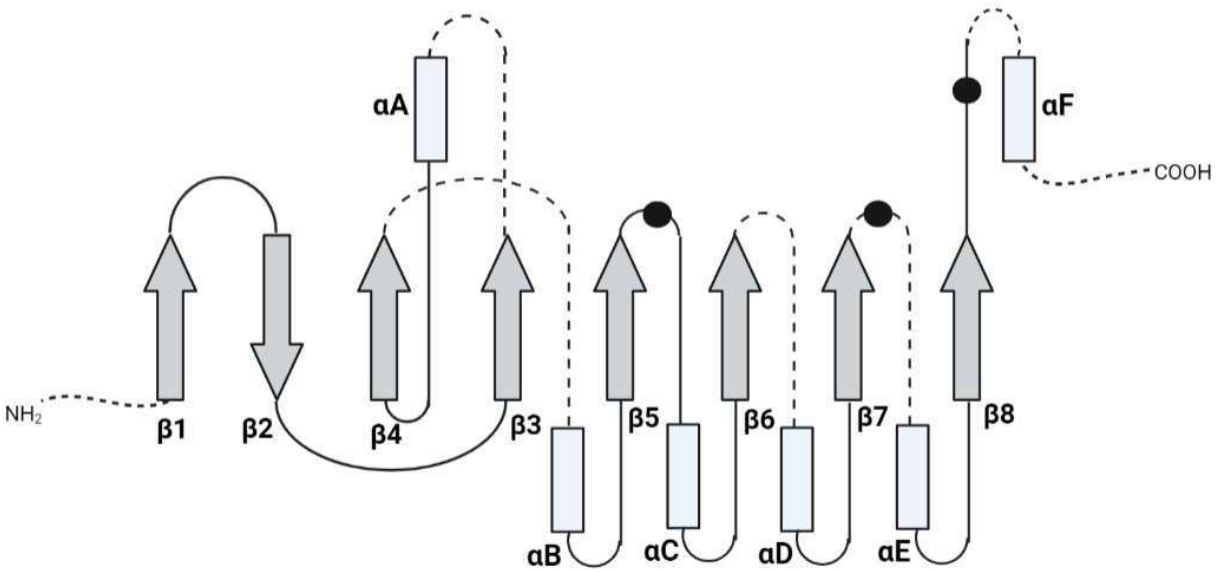

Figure 1.3: Secondary structure diagram of the 'canonical' α/β hydrolase fold. α Helices and β strands are represented by white cylinders and gray arrows, respectively. The location of the catalytic triad is indicated by black dots. Dashed lines indicate the location of possible insertions [16,17]

The nucleophile in the catalytic triad is the central residue for the catalytic reaction. It is mostly serine, but aspartate and cysteine can also take this important role in certain protein structures. The topological location of the nucleophile in the α/β hydrolase fold is the most conserved. It is located between strand β5 and helix C in a sharp ɣ like turn such that the torsion angles (ϕ=-50° and Ψ= -130°) at this residue lie in the unfavorable region of the Ramachandran plot. This sheet-nucleophile-helix turn is called the nucleophilic elbow and is marked by a conserved sequence of residues[14,19]. The helix C is in close proximity with strands β4,β5, and β6, and the sharp turn at the nucleophile can create a steric hindrance. To avoid this, the Nu+2 and Nu-2 residues are mostly amino acids with small side chains (Sm). Therefore, the conserved sequence in all of the α/β hydrolase fold proteins is Sm-X-Nu-X-Sm. Though many variations exist for this sequence, the most commonly occurring sequence is GXSXG, glycine being the simplest amino acid. For similar reasons, the residue at Nu+3 must also have a short side chain, and residues at Nu-4 and Nu-6 must be hydrophobic.

Despite the high structural similarity of the core domain and the catalytic machinery, this huge

superfamily of proteins has diverged to have dissimilar sequences to accommodate for different catalytic and substrate binding activities[20]. This dissimilarity arises from certain added domains and atypical features apart from the conserved catalytically active core domain in many of these enzymes[21,22]. Classification of these enzymes into protein families and provision of structural information has been done and can be accessed by databases like ESTHER and the alpha/beta 3DM database ABHDB[23,24,25].

Many of the proteins in the family were annotated after the identification of the fold and therefore have their nomenclature based on the fold, called the ABHD proteins. The ABHD enzymes, like all the other α/β hydrolase proteins, have the conserved Sm-X-Nu-X- Sm motif, and a few of them have an added acyltransferase activity which is conserved as the His-XXXX-Asp motif [26]. Figure 1.4 shows the phylogenetic relationship and the conserved motifs in each of these proteins.

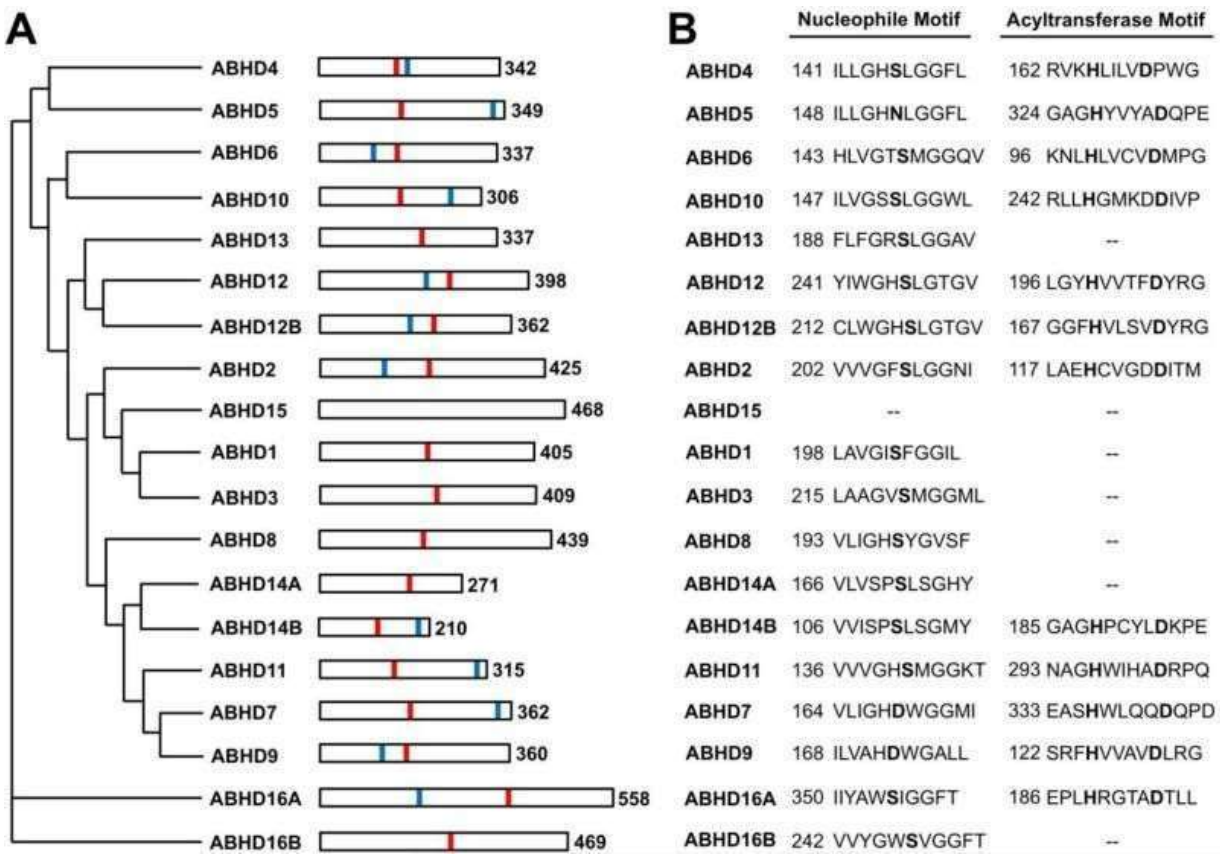

Figure 1.4: The Human ABHD Family. A. Phylogenetic relationship of the human ABHD

proteins based on Clustal W alignment with Poisson correction. The numbers at the right indicate the number of amino acid residues in the full-length human protein. Red lines represent the predicted active site nucleophile, and blue lines indicate the predicted acyltransferase motif (HXXXXD) when present. B. The conserved nucleophilic elbow and acyltransferase motifs. "--"indicates that the motif is not present in the human protein[26].

The various studies on the different ABHD enzymes have emphasized their role in lipid metabolism, glucose metabolism, signal transduction, immunoregulation and therefore implicating their role in various human diseases associated with altered metabolism. Most of these proteins act on endogenous lipids to hydrolyze them, and the products play a role in the regulation of important cellular processes. Their effects on glucose and lipid metabolism have uncovered causal mechanisms for metabolic disease and liver disease development. The metabolic roles of these enzymes have also been shown to aid and/or restrict tumor development in the body. These enzymes also act as effectors in various virus-mediated symptoms. Some of the well characterised examples include:

ABHD1: potential oxidative stress response mediator[27,28]

ABHD2: a novel TAG lipase and ester hydrolase[27,28]

ABHD3: a physiological regulator of medium-chain phospholipids[29]

ABHD4: a principal regulator of N-acylphospholipid metabolism[27,30]

ABHD6: a monoacylglycerol lipase and lysophospholipase[31]

ABHD10: a detoxification enzyme[32]

ABHD11: a diacylglycerol lipase[33]

ABHD12: a brain lysophosphatidylserine and oxidized PS lipase involved in PHARC[48]

ABHD14B: a lysine deacetylase[13]

ABHD16A: a medium and long-chain fatty acid and phosphatidylserine lipase[35,36]

These ABHD proteins have been studied in the past few decades and have shown to have vital roles in mammalian physiology, like any other serine hydrolase. Hence, its only desirable to study the poorly characterized ABHD proteins to gain a better understanding of the primary and secondary metabolism they are involved in. ABHD14A is one such orphan alpha/beta hydrolase domain containing protein with unknown function.

ABHD14A, also referred as DORZ1, is a protein proposed to have a role in cerebellar granule neuron development[36]. It is composed of 271 amino acids in human with a molecular weight of around 30kDa. The gene is located on the p21.2 locus of the human chromosome 3. The catalytic triad is formed by the Ser-171, Asp-222 and His-249 residues, where the nucleophile is present as part of a SPSLS motif. It is assumed to be a type II integral membrane protein, but this is yet to be established.

Background: ABHD14A or Dorz1 was first studied by Hoshino et al. in 2003 when they found that the protein was downregulated in Zic1 deficient mice[36]. Zic1, which is a zinc finger transcriptional regulator protein, is expressed in embryonic neuronal progenitor cells and is documented to control cerebellar granule neuron development by expanding progenitor population and inhibiting differentiation[9]. It has also been reported that Zic1-deficient cerebellum is hypoplastic and lacks a lobule of the anterior lobe. The abnormalities of Zic1-deficient cerebellum could therefore, reflect altered expression status of cerebellar development controlling genes. To investigate these genes, Zic1 was knocked down in mice and a genetic screen was performed against wild type control mice to understand the molecular players involved in cerebellar development. This screening was done at embryonic stage 17.5 (E17.5) since morphological abnormalities in the cerebellum manifest after this stage in the course of development. The most reproducibly downregulated gene from the DNA microarray and RT-PCR experiments was found to be the novel gene, Dorz1[9]. Further RT-PCR experiments revealed that Dorz1 transcript expressed during all developmental stages starting from E12.5, with its peak at E17.5, similar to Zic1. In mice, granule neuron progenitors cover the external surface of the cerebellum, forming the external germinal layer (EGL). They proliferate in the EGL at the perinatal stage. The postmitotic neurons subsequently migrate inward to form the internal granule cell layer (IGL) where they differentiate into the mature granule neurons. In-situ hybridisation experiments showed

coexpression of Dorz1 and Zic1 transcripts in the external germinal layer (EGL) of the cerebellum, with a lower expression of Dorz1 in Zic1 deficient mice at E17.5.

Immunohistochemical analysis also confirmed the colocalisation of both the proteins in the EGL, with Zic1 expressing in the nucleus and Dorz1 antibody staining visible in the cytoplasm of these cells. Further validation for the regulation process was achieved by observing an enhanced Dorz1 expression in cultured cells overexpressing Zic1 protein. Thus, it was concluded that Zic1 positively regulated Dorz1 and through Dorz1, possibly mediated cerebellar granule neuron development (Figure 1.5).

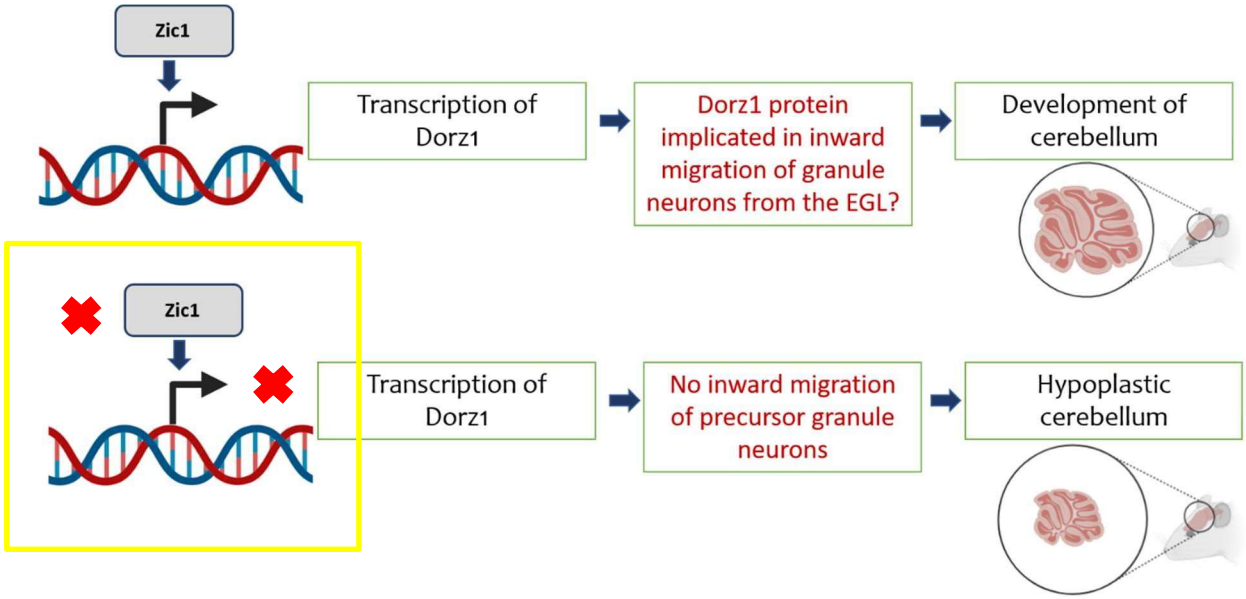

Figure 1.5: Possible role of Dorz 1 in the regulation of cerebellar development

Though the expression profile of Zic1 is localised to the cerebellum, Dorz1 transcripts express ubiquitously in different tissues[37]. This implies that Dorz1 or ABHD14A could be involved in universal metabolic pathways controlling development. ABHD14A has also been reported to be associated with multiple neurodevelopmental disorders like autism spectrum disorder and Williams-Beuren syndrome, with its expression levels altered in such subjects[38,39,40]. Another study on protein structural variants in epileptic patients also showed that this protein might have a role in epilepsy[41]. Studies have also shown that ABHD14A could serve as a prognostic marker for lung and breast cancer[42,43].

Therefore, the study of the enzyme-substrate relationship and protein interactors for this enzyme using biochemical techniques can give deep insights into the metabolic pathways regulated by this enzyme and their manifestation in human physiology and disease.

In this thesis, I try to annotate the biological function of ABHD14A. I try to achieve this goal with advanced chemoproteomics and metabolomic approaches in conjunction with established cell biological and biochemical experiments. In my study, I sought characterisation with first identifying sequence determinants for the efficient annotation of the protein across organismic classes (Chapter 2). I have established protocols for purifying this scarcely researched protein and used chemo proteomic methods to assay its biochemical activity, with emphasis on similar activity on induced expression in cultured cells. I also predict hydrolase activity using preferred substrates. To further investigate the roles of ABHD14A, I developed an antibody against the purified protein and characterised it using different experiments (Chapter 3). I have also performed mass spectrometry-based metabolomics and lipidomics quantifications to fish for any metabolites that might alter their levels due to the activity of the protein (Chapter 4). Overall, using the novel standardised methods for assessing the activity of ABHD14A, I have tried to understand its role in mammalian biochemistry, by probing diverse aspects, including its subcellular localisation, spatiotemporal expression and metabolic changes upon induced expression.

CHAPTER 2:

BIOINFORMATICS STUDIES TO IDENTIFY SEQUENCE AND STRUCTURE DETERMINANTS OF ABHD14A

(A COMPARITIVE STUDY WITH ITS PARALOG ABHD14B)

Enzymes within the Serine hydrolase superfamily have similar overall three-dimensional structures, conserved catalytic residues, but large variations in substrate recognition sites and residues to accommodate the diverse biochemical reactions that are catalyzed within the superfamily.

In an attempt to characterise ABHD14A, we sought out comparative studies with similar and dissimilar sequences and structures within the superfamily, which might give us an idea about probable activity and substrate preference for the protein. Also, since genes with related biochemical pathways express together and are usually clustered together in the genome, to further find associated genes with ABHD14A expression, we also mapped its location in the genome, along with genes that are present around the same locus.

Excitingly, based on this comparative sequence analysis, we found that ABHD14A is closely related to the protein ABHD14B (sequence identity nearly 42%) (Figure 2.1)[44,45]. This is a high number because the globular domains of both the proteins, which are the enzymatic domains have this overlap, which hints to a relatedness. Also, both the genes are present on the same locus on chromosome 3 (p21.2). The transcripts are encoded from complementary strands in the opposite directions (Figure 2.2)[46].

```
CLUSTAL O(1.2.4) multiple sequence alignment


sp|Q9BUJ0|ABHEA_HUMAN      MVGALCGCWFRLGGARPLIPLGPTVVQTSMSRSQVALLGLSLLLMLLLYVGLPGPPEQTS 60
sp|Q96IU4|ABHEB_HUMAN      ------------------------------------------------------------ 0


sp|Q9BUJ0|ABHEA_HUMAN      CLWGDPNVTVLAGLTPGNSPIFYREVLPLNQAHRVEVVLLHGKAFNSHTWEQLGTLQLLS 120
sp|Q96IU4|ABHEB_HUMAN      --MAASVEQREGTIQVQGQALFFREALPGSGQARFSVLLLHGIRFSSETWQNLGTLHRLA 58
                              .       . :   .. .*:**.** .   *..*:****  *.*.**::****: *:

sp|Q9BUJ0|ABHEA_HUMAN      QRGYRAVALDLPGFGNSAPSKEAS--TEAGRAALLERALRDLEVQNAVLVSPSLSGHYAL 178
sp|Q96IU4|ABHEB_HUMAN      QAGYRAVAIDLPGLGHSKEAAAPAPIGELAPGSFLAAVVDALELGPPVVISPSLSGMYSL 118
                           * ******:****:*:*  :   :   * . .::*  .:  **:   *::****** *:*

sp|Q9BUJ0|ABHEA_HUMAN      PFLMRGHHQLHGFVPIAPTSTQNYTQEQFWAVKTPTLILYGELDHILARESLRQLRHLPN 238
sp|Q96IU4|ABHEB_HUMAN      PFLTAPGSQLPGFVPVAPICTDKINAANYASVKTPALIVYGDQDPM-GQTSFEHLKQLPN 177
                           ***     ** ****:** .*:: .  :: :****:**:**: * : .: *:.:*::***

sp|Q9BUJ0|ABHEA_HUMAN      HSVVKLRNAGHACYLHKPQDFHLVLLAFLDHLP    271
sp|Q96IU4|ABHEB_HUMAN      HRVLIMKGAGHPCYLDKPEEWHTGLLDFLQGLQ    210
                           * *: ::.*** ***.**::*  ** **: *
```

Figure 2.1: Sequence alignment of human ABHD14B and ABHD14A(Q9BUJ0: ABHD14A and Q96IU4: ABHD14B)[45]

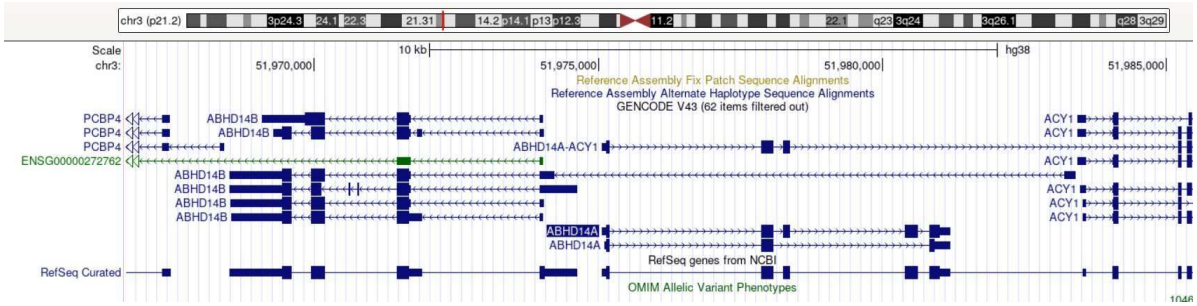

Figure2.2: Concurrent localisation of abhd14a and abhd14b genes on chromosome 3 of the human genome. Image credits: https://genome.ucsc.edu/

Based on their protein sequence, both these enzymes are hypothesized to possess the ABHD-fold, and a conserved catalytic triad (Ser–His–Asp). As compared to other mSHs, the invariant nucleophilic active site serine residue falls within a non-canonical SxSxS motif (canonical motif: GxSxG) (x = any amino acid) for both these enzymes[49]. This distinction makes both ABHD14A and ABHD14B outlying members of the mSH family. Interestingly, unlike any other mSH, both ABHD14A and ABHD14B were discovered from high-throughput screens looking to identify protein interactors of transcription factors. ABHD14A (also known as Dorz1) was found to be a genetic interactor of the transcription factor Zic1, and in mammals, ABHD14A is predicted to have a role in embryonic development of the cerebellum. On the other hand, a yeast two-hybrid screen identified ABHD14B (also known as CCG1-interacting protein B) as a protein interactor of the histone acetyl-transferase domain of the general transcription factor TFIID, and was tentatively assigned a role in transcriptional regulation[47].

Further research has shown that ABHD14B functions as a lysine deacetylase in mammals. Through a series of biochemical and cellular assays, it was found that ABHD14B functions as a novel lysine deacetylase (KDAC)[13]. It was shown that this enzyme transfers an acetyl-group from a post-translationally modified protein lysine residue to a molecule of Coenzyme-A (CoA) to make acetyl-CoA. In a follow-up study, it was found that depleting ABHD14B in mammalian cells and liver of mice results in altered (systemic) glucose metabolism and cellular energetics[50].

We hypothesised that this almost complimentary arrangement of two homologous proteins is unusual and could have implications in their evolution. We used this information to assess

similarities and dissimilarities between ABHD14A and ABHD14B and use these assessments to establish a role for ABHD14A. But, given their high sequence similarity, automated databases often wrongly assign ABHD14A and ABHD14B as the same enzyme, despite being distinct proteins. Therefore, annotating functions to them in various organisms has been problematic. Therefore, we performed a thorough bioinformatics study on both ABHD14A and ABHD14B to identify key sequence determinants for both ABHD14A and ABHD14B and enable better classification for them. Further, we assessed the presence of both these enzymes on the evolutionary time scale and identify protein sequences in various organisms that correspond to either ABHD14A and ABHD14B. Our studies thus pave the way for a better classification of ABHD14A and ABHD14B in an effort toward assigning physiologically relevant functions to them in different organisms in the coming years.

Methods

Bioinformatics searching and analysis: To determine the prevalence of ABHD14A and ABHD14B protein sequences (and its homologues) across all organisms, PSI-BLAST searches[51] were carried out on reference sequences of human ABHD14A (RefSeq: NP_056222.2, Uniprot: Q9BUJ0) and human ABHD14B (RefSeq: NP_001139786.1, Uniprot: Q96IU4), for three iterations, against standard nonredundant databases with an expect threshold of 0.00005 and a maximum return of 5000 hits. To assess the presence or absence of any transmembrane domain(s), all protein sequences from the initial search were submitted to two different transmembrane region prediction software: CCTOP[52] and TMHMM[53]. For additional curation of the data, a home-made script was written to verify the presence of the conserved catalytic triad conserved within the searched motifs across the length of the sequence, by carrying out pairwise global alignments using the Needleman–Wunsh algorithm[54]. For the final resulting of the datasets, a single protein sequence was taken from each representative organism and subjected to a multiple sequence global alignment using MAFFT[55]. The resulting alignments were further assessed in MEGA-X[56] to build maximum-likelihood trees, and the trees were visualized and annotated in iTol[57]. The fully conserved residues for both ABHD14A and ABHD14B were identified using pymsaviz (**pypi.org/project/pymsaviz**/) and Bio.Align (**biopython.org/docs/1.76/api/Bio.Align.html**) packages in Python. The functionally conserved residues for both enzymes were identified by manual inspection of filtered protein sequences and were mapped on structures of each

(ABHD14B structure was derived from PDB:1 imj, ABHD14A structure was derived from AlphaFold).

(The PSI-BLAST searches and tree-building was done by Mr. Golding Rodrigues and the MSA was done by Mr. Archit Devrajan and Sonali Gupta)

Identification of corresponding conserved residues in ABHD14A and ABHD14B: For ABHD14B, after successful examination of the conserved residues on the structure, many of these residues were found to be next to the active site of the domain. These amino acids were recognized, mutated and assessed for change in enzyme activity. The conservation of these residues had been reasoned with appropriate biochemical conjecture (Work by Kaveri Vaidya). We used structures of the proteins and mapped out these residues and checked for conservation of these in ABHD14A, to allow for substrate speculation.

Putative CoenzymeA binding tunnel in ABHD14A: Previous research established ABHD14B as a lysine deacetylase which can transfer an acetyl group from an acetylated lysine-containing peptide to CoenzymeA[13]. Therefore, CoenzymeA is a preferred secondary substrate for the enzyme and the structure must accommodate for this molecule to be accessible to the active site. We used Caver Web 1.0, which is a web server for comprehensive analysis of protein tunnels and channels, and study of the ligands' transport through these transport pathways, to look for a CoA binding tunnel in ABHD14A. we further compared the bottleneck residues that might line the tunnel in both the proteins.

Results

Identification of ABHD14A sequences

The conserved sequence of human ABHD14B has shown that it has the following sequence determinants:

1. Conserved catalytic triad, consisting of Ser-111, Asp-162, and His-188
2. The nucleophilic motif (consisting of a SxSxS motif within the VVISPSLSGMY sequence, x = any amino acid)

3. ABHD14B acyltransferase motif (consisting of the HxxxxD motif within the GAGHPCYLDKPE sequence, x = any amino acid) toward the C-terminal end of the protein.

Owing to its high sequence similarity to ABHD14B, various bioinformatics studies have predicted that the three-dimensional structure of ABHD14A also has an ABHD-fold, and possesses a conserved catalytic triad, consisting of Ser-171, Asp-222, and His-249 for the human ABHD14A sequence. Like ABHD14B, bioinformatics studies with other ABHD-proteins from the mSH family have identified a conserved nucleophilic motif (consisting of a SxSxS motif within the VLVSPSLSGHY sequence, x = any amino acid) . Of note, sequence analysis suggests that ABHD14A lacks the acyltransferase motif seen in ABHD14B, and unlike ABHD14B, surprisingly, has an integral membrane domain consisting of ~30–40 amino acids that form an anchoring α-helical sequence at the N-terminal end of the protein (Figure 2.3).

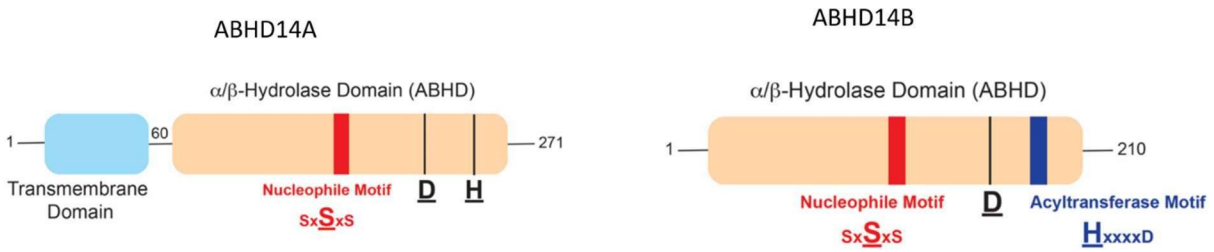

Figure 2.3: Schematic representation of the human ABHD14A and ABHD14B structure. Based on available literature, ABHD14 proteins contain the catalytic triad consisting of Ser-Asp-His, and a nucleophilic motif that contains the active site serine residue as part of a SxSxS sequence within an overall ABHD-fold. In addition, ABHD14A contains a N-terminal domain that is predicted to anchor it to the cellular membranes. ABHD14B contains an additional acyltransferase motif.

Of the 5000 hits obtained from using human ABHD14A (RefSeq: NP_056222.2, Uniprot: Q9BUJ0) as a query sequence for search, the nucleophilic motif for ABHD14A was identified in 733 sequences (allowing for up to two mismatches), of which 134 sequences were perfect matches, while the catalytic triad was identified in 2624 sequences. From the 5000 hits obtained from the initial search, the two transmembrane prediction software, CCTOP and TMHMM, predicted transmembrane regions in 1069 and 1084 sequences, respectively. Of these, a total of 1010 sequences were common to both prediction software, while 129 were identified by a single software, leading to a complete set of 1139 protein sequences with an identified transmembrane region. Based on the above information, in our study, a protein sequence was classified as ABHD14A, if it possessed the catalytic triad, the ABHD14A nucleophile motif

(allowing for up to two mismatches), and had a transmembrane domain. Based on this filtering criteria, overall, we identified 483 ABHD14A sequences identified from 312 organisms, of which 116 ABHD14A sequences identified from 52 organisms were perfect matches to the aforementioned filtering criteria.

Phylogenetic classification of ABHD14A sequences: Upon applying the aforementioned filtering criteria for the shortlisted ABHD14A sequences obtained from various databases, we identified 483 ABHD14A sequences from 312 organisms. Upon manual curation of these data, it was clear that several organisms (especially from class *Mammalia* and *Actinopterygii*) possessed more than 1 isoform of ABHD14A, and therefore, there was a disconnect between the total ABHD14A sequences and the organisms identified from our search. Next, we chose the longest ABHD14A sequence from any particular organism to perform a phylogenetic (evolutionary) analysis for ABHD14A, and found that ABHD14A was largely confined to phylum *Chordata* (~97.5%, 304 organisms of the 312 organisms identified), with a smaller representation from the *Arthropoda, Amphibia* and *Cnidaria* phyla. Among the phylum *Chordates*, the ABHD14A sequences were predominantly found in class *Mammalia* (Mammals) (~58%, 182 organisms of the 312 organisms identified) and *Actinopterygii* (Bony Fish) (~37%, 114 organisms of the 312 organisms identified), with a much smaller representation seen in *Reptilia* (Reptiles) (~2%, 6 organisms of the 312 organisms identified). The phylogenetic analysis showed that within the *Chordates*, the ABHD14A protein sequences from class *Actinopterygii* and *Mammalia* were most closely related to one another, and together were related to ABHD14A sequences from the class *Reptilia*. Of the 312 organisms that we identified possessing a ABHD14A sequence, 263 organisms also possessed an ABHD14B sequence, an overall fraction (~84% of the total organisms) far greater than ~38% observed from the earlier ABHD14B analysis (Figure 2.4).

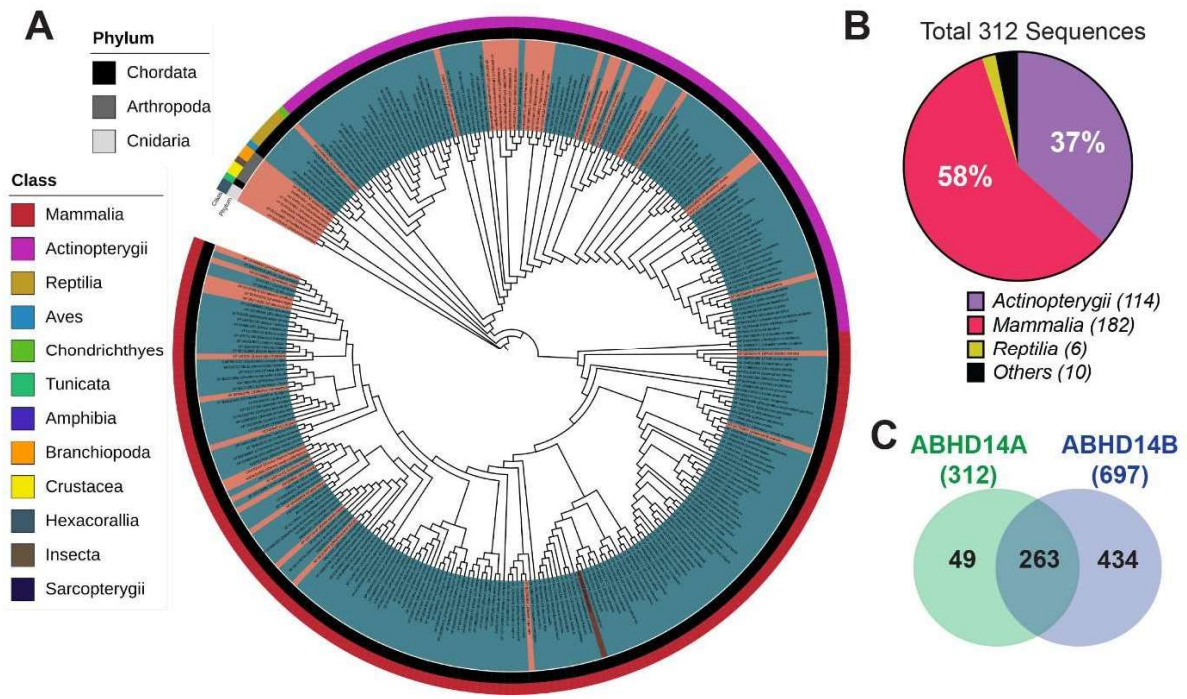

Figure 2.4: Phylogenetic analysis of ABHD14A sequences. (A) Phylogenetic tree representing the identified ABHD14A sequences from 312 organisms. The outermost and middle circular coloring denotes the Class and Phylum to which an ABHD14A sequence belongs (see associated legends within the figure), while the innermost circular coloring (orange or teal) denotes whether an organism contains a sequence only for ABHD14A (orange) or for both ABHD14B and ABHD14A (teal). (B) Pie-chart analysis representing the data from the phylogenetic tree for the various classes of organisms, mainly from Chordates that contain an ABHD14A sequence. This analysis shows that class Mammalia and Actinopterygii contain the most sequences for ABHD14A within the Chordates. (C) Venn diagram showing the overlapping number of organisms that contain ABHD14A and ABHD14B sequences among those identified from the bioinformatics analysis.

The most striking and surprising aspect of this phylogenetic analysis for ABHD14A was that based on our filtering criteria, we failed to identify any ABHD14A sequences from class *Aves* within the *Chordates*. This runs counter to the fact that *Aves* possessed the highest number of sequences for ABHD14B, suggesting that there might be three broad possibilities: (i) Perhaps our filtering criteria for identification of ABHD14A were too stringent; and/or (ii) *Aves* did not possess sequences for ABHD14A (lost during evolution); and/or (iii) ABHD14A sequences possessed by *Aves* were very distinct from ABHD14A sequences identified from other organisms. To exclude, possibility (i), we re-searched the 5000 hits, lowering the mismatch threshold to three and four mismatches, and were still unable to identify any ABHD14A sequences from *Aves*. Our current studies therefore, cannot exclude the

possibilities (ii) and (iii), and further bioinformatics analysis for ABHD14A sequences specific to class *Aves* will be needed to resolve this preliminary yet interesting finding.

Conservation of residues within the ABHD14A sequences: To assess the overall conservation in protein sequence for ABHD14A, we performed a multiple sequence alignment analysis on all the 312 sequences identified for ABHD14A from different organisms. Here, we found that from the 312 ABHD14A sequences, 99 residues were highly conserved (present at a frequency of >90% in all the 312 ABHD14A sequences at the defined position), suggesting that across all organisms, the overall sequence conservation is fairly high (~40%). In addition, upon closer inspection, for ABHD14A sequences, we found that within a particular class (e.g., *Mammalia*), the extent of sequence conservation was significantly higher. Besides the conserved residues, we found that 50 residues were functionally conserved for the 312 ABHD14A sequences, suggesting that the overall sequence conservation across all organisms for ABHD14A was realistically ~60% (Figure 2.5) .

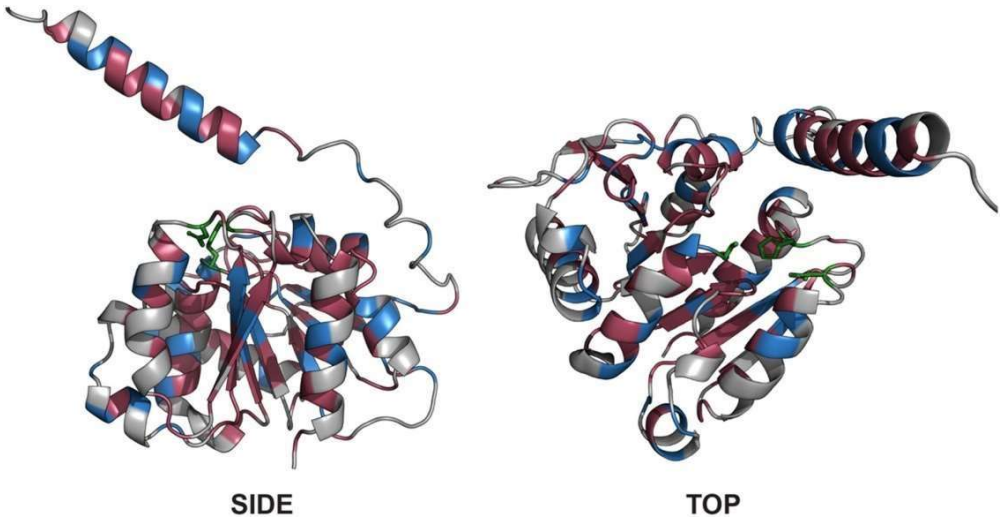

Figure 2.5: Mapping conserved residues on the ABHD14A structure. The residues colored in red are those that are absolutely conserved, while those shown in blue are functionally conserved based on the multiple sequence alignment analysis across all the 312 sequences of ABHD14A from different organisms. The catalytic triad residues that mark the active site are shown in green.

Mapping of conserved residues on the ABHD14A predicted structure: We wanted to map the conserved residues identified for ABHD14A to a three-dimensional protein structure. However, in the absence of any available ABHD14A structure, we used an AlphaFold Protein Structure Database predicted structure of human ABHD14A (Uniprot ID: Q9BUJ0). To ensure that this structure was useful for further analysis, we first overlaid this AlphaFold-generated

structure of human ABHD14A[58, 59], with the crystal structure of human ABHD14B (PDB: 1imj). From this structural analysis, we found an almost perfect overlay of the ABHD-fold portion of ABHD14A with the overall structure of ABHD14B (Figure 2.6). In fact, the catalytic triad that comprises the active site of both these enzymes showed near identical orientations and gave us confidence that the overall predicted structure of human ABHD14A would be useful for our structural analysis. Interestingly, the N-terminal region of the predicted human ABHD14A structure showed both an extended disordered stretch and an α-helical region that presumably anchors this enzyme to a cellular membrane. Finally, we mapped all the conserved residues on the AlphaFold predicted structure of human ABHD14A and found that these conserved residues (including functionally conserved residues) were clustered around the enzyme active site (catalytic triad) and the cleft adjoining this active site where the putative substrates of this enzyme are predicted to bind. Further, we also found from this structural analysis that the residues present on the α-helical region at the N-terminus of the protein that is predicted to be involved in membrane anchoring of ABHD14A were also highly conserved.

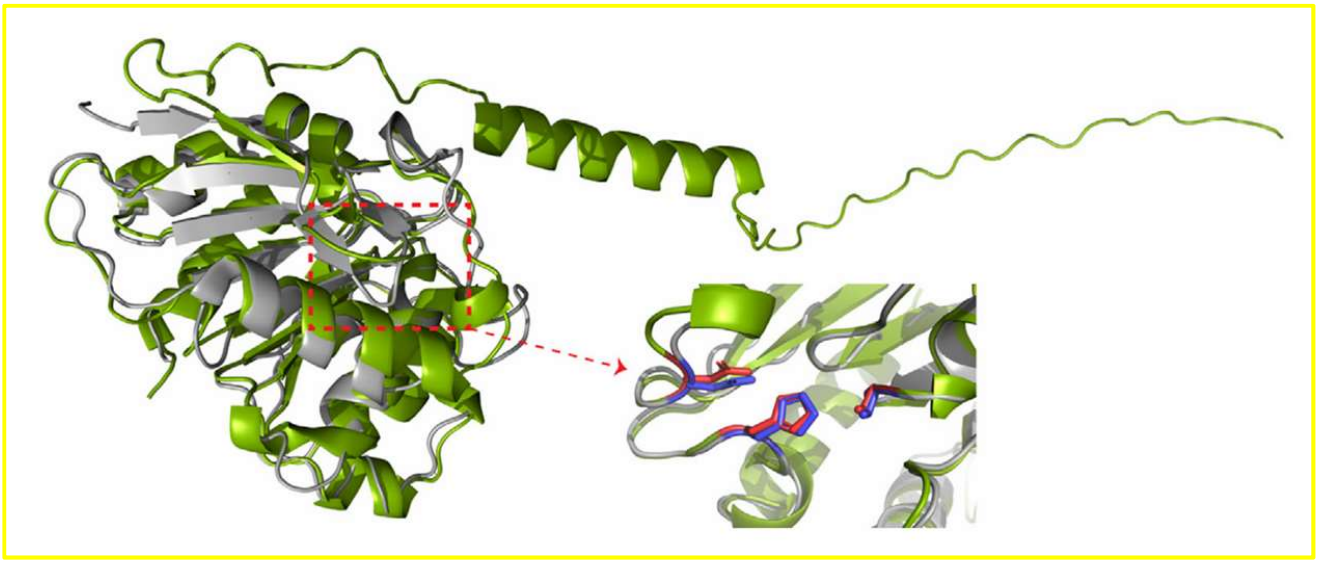

Figure 2.6: Overlay of the human ABHD14A and human ABHD14B structures. Superimposition of the AlphaFold predicted structure of human ABHD14A (Uniprot ID: Q9BUJ0) (green structure) with the three-dimensional crystal structure of ABHD14B (PDB: 1 imj) (gray structure) showing an almost perfect overlay of the ABHD-fold region of both proteins. A zoomed image of the catalytic triad also shows that these residues are perfectly aligned in both structures (blue residues for ABHD14B and red residues for ABHD14A). The ABHD14A predicted structure shows an additional N-terminal region that comprises of an α-helix, that is responsible for membrane anchoring of this enzyme.

This is interesting, because unlike the cellular localization of ABHD14B (cytosolic and nuclear), ABHD14A might be localized to the plasma membrane or microsomal components (e.g., Golgi, endoplasmic reticulum, peroxisome), and may have functions that are quite distinct from ABHD14B. While only speculative based on the bioinformatics data, this premise however needed to be experimentally validated. Also of note and biological importance is that despite the high overall sequence similarity (~40%–50%) of ABHD14A and ABHD14B within a particular organism that possesses both enzymes (e.g., humans), it is interesting to note that ABHD14A lacks the acyltransferase motif. This implies that unlike the ABHD14B, perhaps ABHD14A performs a function distinct from the known acyltransferase-type activity of ABHD14B.

Identification of conserved residues important for ABHD14B function: The following list of residues were mapped to be of importance for the activity of ABHD14B:
The important residues of ABHD14B were identified by looking for the 90% functionally conserved residues, which were mapped onto the structure. Important residues were further picked based on their predicted importance in the structure and/or functions.

Residue	**Possible chemistry**
R42	Present close to the active site, might interact electrostatically with the substrate.
H55, R56, H199	Present in the CoA tunnel, might be involved in pyrophosphate charge neutralisation
S75	Fully conserved residue near the surface, might be a site for PTM
K141	Predicted to interact electrostatically with the substrate
Y191, W198	Found in the CoA binding tunnel and might be involved in pi stacking with CoA
D193	Part of the acyl transfer motif
D162A, H188A	Part of the catalytic triad

Structural overlay using PyMol revealed that many of these important residues for ABHD14B activity were not conserved in the sequence of ABHD14A, implying diverging roles for the proteins in terms of substrate preference and activity (Figure 2.7).

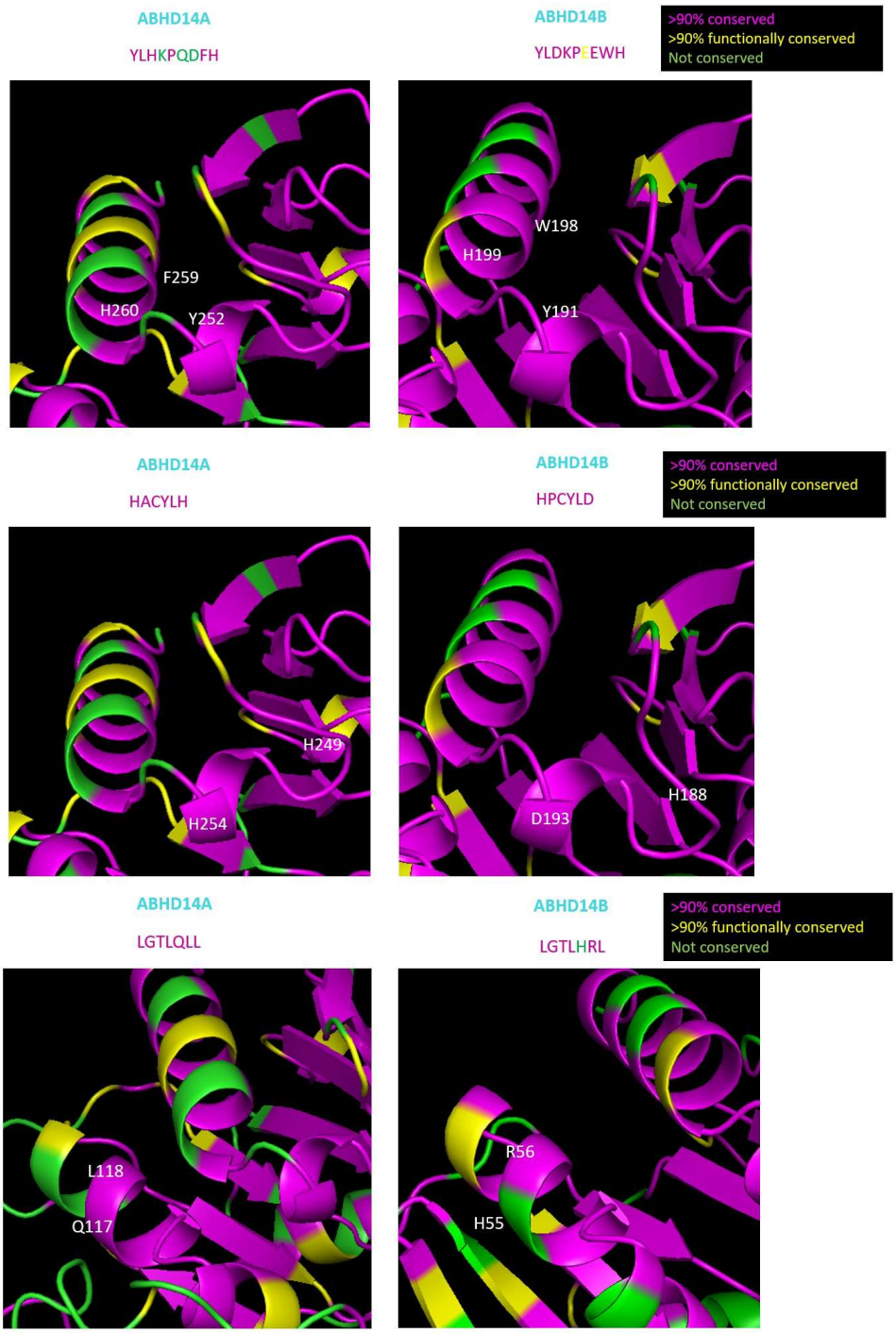

Figure 2.7: Sequence and structural comparison between ABHD14A and ABHD14B show that important motifs for ABHD14B activity are not simulated in the sequence and structure of ABHD14A.

Predicted CoA binding tunnel is absent from ABHD14A: We used the alphafold structure of the human ABHD14A to predict potential tunnels in the structure of the protein, using the CAVER web tool. The combined length of the calculated tunnel must be approximately 20 Å, which is appropriate for binding the phosphopantetheine arm of CoA. But our analysis with ABHD14A revealed a tunnel as long as 4 Å (Figure 2.8).

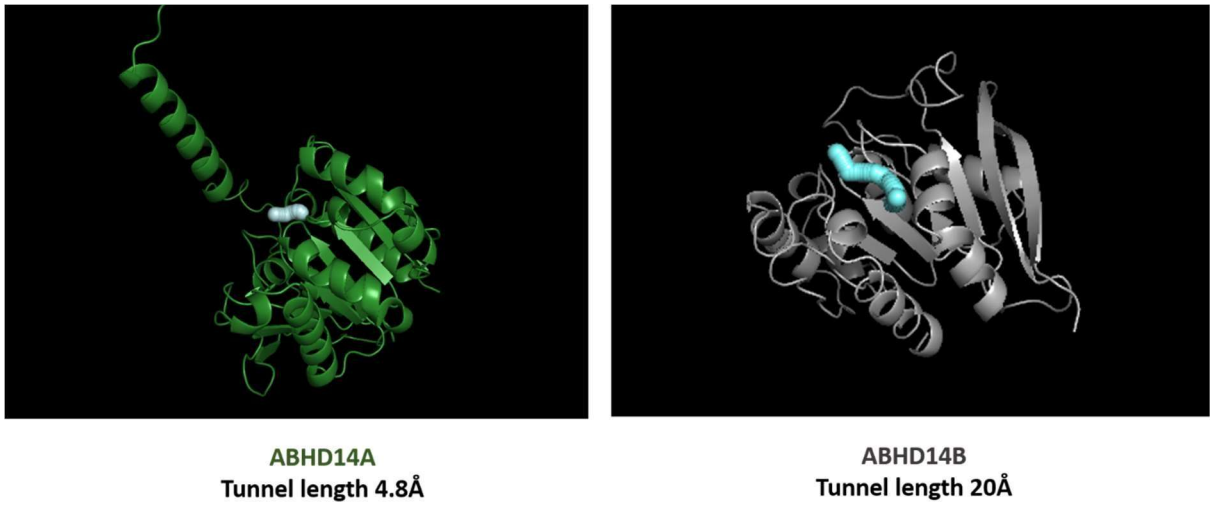

Figure 2.8: Prediction of CoenzymeA binding tunnel (20 Å) in the structures of ABHD14A and ABHD14B using the CAVER web tool. ABHD14A does not show any tunnel that could bind to Coenzyme A based on the prediction.

To validate this prediction, we aligned the sequences of ABHD14A and ABHD14B to compare the bottleneck residues of the CoA binding tunnel in ABHD14B to corresponding residues in ABHD14A. Bottleneck residues are amino acids that limit the access of the substrate to the enzyme and ensure strong binding. We found that most bottle neck residues were identical in the two proteins but the residues adjacent to the bottleneck residues had very different properties. This difference in amino acids lining the tunnel might affect the availability of channels for the binding of CoA and therefore, an impairment in the detection of the tunnel (Figure 2.9).

A

Tunnel analysis using CAVER web tool

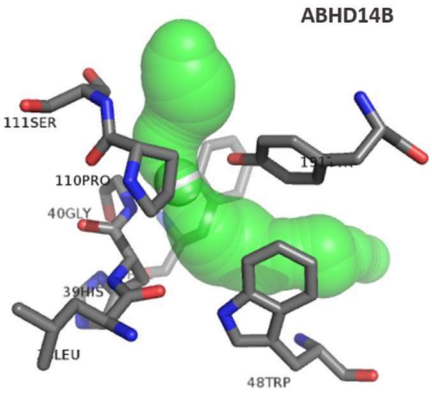

C

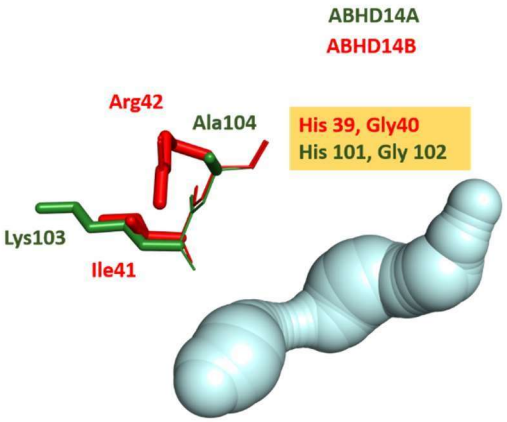

B

Coenzyme A tunnel lining residues

Bottleneck residues

Different residues

ABHD14A	ABHD14B
Leu100	Leu38
His101	His39
Gly102	Gly40
Lys103	Ile41
Ala104	Arg42
Phe105	Phe43
Ser107	Ser45
His108	Glu46
Thr109	Thr47
Trp110	Trp48
Glu111	Gln49
Gln112	Asn50
Leu113	Leu51

ABHD14A	ABHD14B
Thr115	Thr53
Pro170	Pro110
Ser171	Ser111
Leu172	Leu112
Ser173	Ser113
Ile194	Val134
Ala195	Ala135
Pro196	Pro136
Asp222	Asp162
His249	His188
Ala250	Pro189
Leu251	Leu190
Tyr252	Tyr191

Figure 2.9: Comparison of residues lining the Coenzyme A binding tunnel in ABHD14A and ABHD14B. (A) Representative image of the CoenzymeA binding tunnel in ABHD14B lined by the bottleneck residues. (B) List of CoenzymeA lining residues in ABHD14B and their corresponding residues in ABHD14A. The bottleneck residues are shaded in yellow and the adjacent residues are shaded in pink. (C) Representative image of the effect of surrounding residues on the availability of bottleneck residues and hence, the disruption of the Coenzyme A tunnel in ABHD14A. Alanine and Lysine (ABHD14A) have very different properties as compared to Arginine and Isoleucine (ABHD14B).

Discussion

ABHD14A is not the typical alpha/beta hydrolase domain containing protein where the canonical GXSXG motif is found to accommodate the active site serine. It also has an N-terminal transmembrane alpha helix of around 20 amino acids. The sequence annotation of the protein becomes more confusing as we expand the knowledgebase to multiple organisms. This is because of two specific reasons: atypical sequence determinants for a serine hydrolase and the misassignment of sequences to its paralog protein ABHD14B. This misassignment is common due to the high sequence similarity between the two proteins (42 percent) and their incomplete characterisation over the years.

As part of this chapter, we have tried to use phylogenetic analysis to assign sequences in most classes of organisms in either category of the proteins. This enables us and many other people to use this data as a knowledgebase for further studies. In an attempt to make this classification, we also put out some clear determinants of protein identity for both the paralogs, which can be used for any sequence henceforth. This phylogenetic analysis helped us understand that the two proteins possibly evolved in a divergent manner. This is also corroborated with their gene presence on the opposite strands of the same locus. This has possible happened due to a gene duplication event over the course of time. We could not map any sequence in birds that matched our criteria to label it as ABHD14A, which is an interesting observation to further look into. We also identified conserved residues in both the protein structures that could aid us in recognizing conserved regions in the structure that might be helpful in substrate binding. Such regions were identified for ABHD14B. So we used a comparative analysis to see if similar domains exist for ABHD14A and we found considerable differences in the amino acid composition. We also tried to map out a CoenzymeA binding tunnel in ABHD14, as was predicted for ABHD14B, but the sequence differences implied that such a tunnel might not exist in the native structure. If at all, ABHD14A also binds to CoenzymeA, this could be due to conformational changes due to binding to a cofactor or due to a signalling response. Overall, this chapter focuses on the key similarities and dissimilarities between the two ABHD14 proteins that aid in understanding the biophysical characteristics of ABHD14A better.

CHAPTER 3

BIOCHEMICAL CHARACTERISATION OF ABHD14A AS AN ACTIVE SERINE HYDROLASE

The alpha/beta hydrolase domain containing protein 14A (ABHD14A) was first identified as the Dorz 1 protein in a study that looked for mediator genes and their protein products that regulate cerebellar development through the activity of the Zic1 transcription factor. There are multiple other studies that imply that the gene for ABHD14A is a well-established candidate responsible for several neurodevelopmental disorders (genomic mutations, transcription clusters, altered levels of the transcript etc). The transcript is ubiquitously expressed across different tissues (also cell lines), with maximum expression in brain. Protein databases identify the translational product as a transmembrane domain containing protein with the alpha/beta globular domain. The hydrophobicity index of the transmembrane domain (around 20-30 residues) at the N-terminus was calculated using the TMEM prediction tool. The human ABHD14A protein is 271 amino acids long with the following predicted catalytic triad: Ser 171-Asp 222- His 249. The expected size of the protein is 30kDa and its predicted to have a vesicular localisation within the cell.

Most studies that have shown the involvement of ABHD14A in different physiological aspects, have focused on the genetic or transcript form of regulation. There are no absolute studies on the translated product of the gene and therefore, the protein is not characterised very well in terms of its biochemistry. This is further exemplified with the absence of any databases that talk about its expression pattern across different tissues and cell line and the lack of an efficient antibody against the protein.

In order to characterise ABHD14A protein, we standardised methods for purifying this scarcely researched protein. We recombinantly purified a truncated variant of human ABHD14A from *E. coli*, and biochemically assayed this enzyme. We demonstrated using gel-based ABPP and colorimetric assays, that human ABHD14A is indeed an active enzyme, capable of hydrolysing p-nitrophenyl-esters. We also show that human ABHD14A possesses an acetyltransferase activity with Coenzyme A (Co-A) being the other substrate, and acetyl-Co-A being the product of this biochemical reaction. To investigate the expression of ABHD14A in mammalian cells and tissues, we developed a polyclonal anti-ABHD14A antibody, and show contrary to publicly available databases, that most immortalized cell lines and adult mouse tissues lack

ABHD14A expression. Finally, we overexpressed full length ABHD14A in HEK293T cells, and showed that this enzyme is active in mammalian cells and is sub-cellularly localized to the Golgi. Overall, using the novel standardised methods for assessing the activity of ABHD14A, we have tried to understand its role in mammalian biochemistry, by probing diverse aspects, including its subcellular localisation and spatiotemporal expression. Therefore, our studies provide the first evidence of any activity for this cryptic enzyme, and open new avenues to study this poorly characterized enzyme in the context of mammalian physiology.

We have used two major techniques to annotate the protein as a Serine hydrolase. The first is Activity Based Protein Profiling (ABPP)[60]. This is a technique in which reporter-tagged activity probes that react covalently and irreversibly only with the active form of serine hydrolases can be used to profile the pattern of serine hydrolase activity by gel-based ABPP. The small molecule probe called an activity-based probe (ABP) is made up of three parts – the functional warhead, the linker and the reporter tag. A commonly used ABP for serine hydrolases is Fluorophosphonate-Rhodamine, wherein the active site serine irreversibly binds to the FP moiety (Figure 3.1).

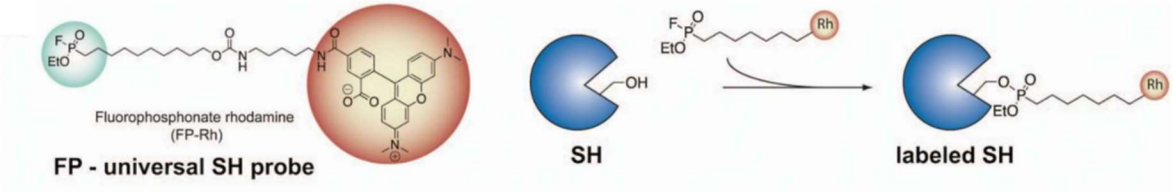

Figure 3.1: Fluorophosphonate-Rhodamine is used as an activity-based probe, which covalently labels all active serine hydrolases[60].

The second is para-nitro phenol acetate hydrolysis assay. This is a colorimetric assay which measures the formation of product (para-nitro phenol) by measuring absorbance at 405nm[61]. The conversion of para-nitrophenol-acetate to para-nitro phenol in the presence of an enzyme, is an indication of its hydrolase activity.

Materials: All chemicals, buffers, and reagents were purchased from Sigma-Aldrich, and all tissue culture media and consumables were purchased from HiMedia, unless mentioned otherwise.

Methods:

Cloning and expression of recombinant human ABHD14A in *E. coli*: The wild type (WT) human *abhd14a* gene (UniProt ID: Q9BUJ0) was synthesized from GenScript as a codon-optimized construct for expression in *E. coli*. The human ABHD14A contains 271 amino acids, including an approximately 60-residue N-terminal transmembrane segment. We tried cloning a series of constructs with different tags (GST, SUMO-His and MBP) to optimize the expression and solubility of the protein, but the recombinant protein was highly unstable (Table 3.1). Because full-length protein expression and purification was unsuccessful, a series of N-terminally truncated constructs (successive 10-aa deletions) bearing an N-terminal 6X-His tag were cloned into the pET45b(+) vector (Millipore). Recombinant plasmids were transformed into *E. coli* BL21(DE3). Cells were lysed in 1X-phosphate buffered saline (PBS), and soluble and membrane fractions were separated by centrifugation (21,000g, 4 ^{o}C, 45 min). Equal protein amounts from each fraction were analysed by SDS-PAGE to evaluate expression and solubility.

Fusion protein construct	**Expression**	**Purification**	**Biochemical activity**
C-His, N-His ABHD14A	Membrane-very low	Unsuccessful	-
N-GST ABHD14A	Membrane- low	Successful	Unsuccessful
N-MBP, C-His ABHD14A	Membrane-low	Unsuccessful	-
N-His, SUMO ABHD14A	Membrane-low	Successful	Unsuccessful

Table 3.1: List of constructs cloned for the expression and purification of recombinant ABHD14A. The table also lists the efficiency of each construct for expression, purification and activity assessment assays.

Purification of NΔ60-ABHD14A variants: *E. coli* BL21(DE3) containing the N-terminal 6X-His tagged NΔ60-WT ABHD14A construct was grown in LB medium with 100 µg/mL ampicillin at 37 ^{o}C with constant shaking. At an optical density of 0.6 at 600 nm (OD_{600} ~ 0.6),

protein expression was induced by adding 100 μM isopropyl-β-*D*-1-thiogalactopyranoside and reducing the temperature to 18 °C for 16 h. Cells were harvested by centrifugation (6000 rpm, 20 min, 4 °C) and resuspended in lysis buffer (50 mM Tris, 50 mM imidazole, 500 mM NaCl at pH 8.0). Lysates were prepared by sonication, and clarified by centrifugation (15,000g, 4 °C, 45 min). The resulting soluble fraction was applied to a Ni^{2+}-NTA affinity column (GE Healthcare), which was pre-equilibrated with the lysis buffer. The protein bound to the column was eluted with an elution buffer (50 mM Tris, 250 mM imidazole, 500 mM NaCl at pH 8.0) as per manufacturer's instructions. Eluted fractions were dialyzed in the assay buffer (50 mM Tris, 500 mM NaCl at pH 8.0) to remove excess imidazole, flash-frozen in liquid nitrogen, and stored at −80 °C until further use. A catalytically inactive S171A variant of ABHD14A (N-terminal 6X-His tagged ΔN60-S171A ABHD14A) was generated using site directed mutagenesis (New England Biolabs) as per manufacturer's instructions and purified using the procedure mentioned above. Protein purity was assessed by SDS-PAGE analysis, and concentrations were determined using the Bradford assay.

Gel based ABPP assays of the NΔ60-ABHD14A variants: All gel-based ABPP assays were done as per procedures previously reported by us, using the fluorophosphonate-rhodamine (FP-rhodamine) probe. For protein titrations, the NΔ60-ABHD14A variant (WT and S171A) concentrations ranged from 2 to 10 μM, with a constant FP-rhodamine concentration of 5 μM. For probe titration experiment, the NΔ60-ABHD14A variant (WT and S171A) concentration was maintained at 2 μM, and FP-rhodamine concentrations varied from 0.2 to 5 μM. Samples were resolved by 10% SDS-PAGE and the in-gel fluorescence of the probe-labelled proteins was visualized on the iBright1500 gel documentation system (Invitrogen). All gels were subsequently stained with Coomassie Brilliant Blue to confirm appropriate protein loading.

p-Nitrophenyl-ester hydrolysis assays of the ΔN60-ABHD14A variants: All p-nitrophenyl-ester assays was performed using substrates and procedures mentioned earlier, and the release of p-nitrophenol from the p-nitrophenyl-ester was monitored at 405 nm. A typical p-nitrophenyl-ester hydrolysis reaction was performed in a 250 μL volume, contained 10 μM NΔ60-WT ABHD14A [native or heat denatured (negative control)] and 500 μM p-nitrophenyl-ester in the assay buffer. To determine the effect of Co-A or Acetyl-Co-A on the rate of p-nitrophenyl-ester hydrolysis, NΔ60-WT ABHD14A (10 μM) was incubated with Co-A (1 mM)

or Acetyl-Co-A (1 mM) at 37 ºC for 15 min, and the reaction were initiated by adding 50 μM p-nitrophenyl-ester under assay conditions previously reported.

Production of an ABHD14A antibody: The anti-ABHD14A primary antibody was generated in rabbits using the purified human NΔ60-WT ABHD14A as the antigen in the National Facility for Gene Function in Health and Disease (NFGFHD) at IISER Pune using in house protocols [Formal approval from the IISER Pune – Institutional Animal Ethics Committee (IISER-P IAEC) (protocol no: IISER_Pune/ IAEC/2021_01/08 and IISER_Pune/ IAEC/2023_01/05)]. Briefly, a female New Zealand rabbit was immunized with 0.3 mg of purified human NΔ60-WT ABHD14A emulsified in Complete Freund's Adjuvant (day 0). Thereafter, post-immunization, booster doses were administered on days 14, 42, 70 and 98. The serum was collected 14 days after each booster dose and terminally on day 126. The antibody titres from the harvested sera were evaluated against the antigen (0.01 to 1 μg) using established Western blot analysis procedures. The anti-ABHD14A antibody was purified via affinity chromatography by covalently coupling the antigen as a bait on a SulfoLink resin (buffer used: 50 mM Tris, 5 mM EDTA at pH 8.5). Following coupling and cysteine blocking, the resin was washed extensively, first with 1 M NaCl and subsequently with 20 mM Tris at pH 7.5. The bound anti-ABHD14A polyclonal antibodies were eluted using 100 mM glycine (pH 2.5) in 500 μL fractions, neutralized, pooled, and dialyzed into storage buffer [50% (v/v) glycerol, PBS, 0.2% (w/v) sodium azide]. The antibody performance was validated at a dilution of 1:1000 against various amounts of the antigen (0.01 to 1 μg) relative to a commercially available antibody (Sigma-Aldrich; catalog no: SAB4501087) by Western blotting experiments. Typically, around 30μg of proteome is loaded on an SDS-PAGE gel of appropriate percentage. The protein is transferred on to a nitrocellulose membrane in transfer buffer (25mM Tris-HCl, 192mM glycine, pH 8.3, in 20% methanol(v/v)) at 90V for 90 mins. Later, the membrane is blocked with Blocking buffer (5% skimmed milk in PBST (PBS with 1% Tween 20(v/v))) for 1 hour at room temperature. The membrane is then incubated with an appropriate dilution of primary antibody in blocking buffer for 12-16 hours at 4 ºC. This is followed by 3 washes with PBST for 10 mins each, incubation with secondary antibody at appropriate dilution in blocking buffer at room temperature and then repeating the same cycle of washes. The blot is finally developed using luminol and HRP solution. Ponceau staining is alternatively performed before blocking to look for appropriate transfer of all proteins.

ABHD14A expression in immortalized cell lines and mouse tissues: The expression of ABHD14A in various mammalian cell lines or adult mouse tissues was assessed using Western blot analysis using established protocols. Briefly, lysates (50 μg) from several immortalized mammalian cell lines (A549, BV2, HEK293T, HeLa, HepG2, Neuro2A, NIH3T3, RAW264.7, THP-1) or adult mouse tissues (brain, heart, liver, lung, kidney, muscle, pancreas, spleen, testis) were analysed by Western blot analysis using our in house anti-ABHD14A antibody or a commercially available anti-ABHD14A (Sigma-Aldrich; catalog no: SAB4501087) at a dilution of 1:500. In these immunoblotting experiments, 0.05 μg of purified human ΔN60-WT ABHD14A was used as a positive control, and Ponceau staining was used to ensure appropriate protein loading.

Overexpression of rat ABHD14A variants in HEK293T cells: The full length WT rat ABHD14A (UniProt ID: Q5I0C4) cloned in the pCMV-Sport6 mammalian expression vector was purchased from GE Dharmacon (now Horizon Discovery), and the catalytically inactive S142A variant was generated in the same vector using the site directed mutagenesis strategy (New England Biolabs) as per the manufacturer's instructions. The rat ABHD14A variants were overexpressed in HEK293T cells using the Lipofectamine 2000 (Thermo Fisher Scientific) via a transient transfection strategy. Briefly, HEK293T cells were cultured in Dulbecco's Modified Eagle Medium (DMEM) containing 5% (v/v) fetal bovine serum and 1% (v/v) penicillin–streptomycin till 60% confluency. At this confluence, the cells were transfected with DNA (10 μg) in a 1:4 DNA:Lipofectamine ratio in OptiMEM media (Thermo Fisher Scientific), incubated for 45 min prior to addition to cells. Post-transfection, the media was replaced after 12 h, and cells were harvested after 60 h. Lysates were prepared by sonication in PBS, and soluble and membrane fractions were separated by centrifugation (21,000g, 4 °C, 45 min). Gel-based ABPP analysis were performed on the membrane lysates (40 μg) from ABHD14A-transfected or mock-transfected HEK293T cells using FP-rhodamine (10 μM) as per protocols previously reported. Overexpression of ABHD14A variants in HEK293T cells was confirmed by Western blot analysis using anti-ABHD14A antibody (rabbit; in house antibody or Sigma-Aldrich; catalog no: SAB4501087; 1:1000 dilution) (primary antibody) and HRP-conjugated anti-rabbit antibody (Goat IgG) (Invitrogen; catalog no: 31460; 1:10000 dilution) (secondary antibody) as per protocols previously reported.

Cellular localization of ABHD14A: The subcellular localization of ABHD14A was assessed in HEK293T cells transfected with full length WT rat ABHD14A, where mock-transfected cells were used as controls. The cells grown on coverslips were fixed with 4% (w/v) paraformaldehyde in 1X PBS for 15 min and permeabilized with 0.05% (w/v) Triton X-100 in PBS for 15 min. The cells were subsequently blocked with blocking buffer (5% (w/v) BSA in PBS) for 30 min, followed by probing with the following primary antibodies: anti-ABHD14A antibody (rabbit; in house antibody or Sigma-Aldrich; catalog no: SAB4501087; 1:100 dilution), and anti-GM130 antibody (BD Biosciences, catalog no: 610822; 1:100). This was followed by 3*5 minutes washes with PBS. The secondary antibodies used in this study were: Alexa Fluor-633 anti-rabbit IgG (Invitrogen; catalog no: A21070; 1:1000) and Alexa Fluor-568 anti-mouse IgG (Invitrogen; catalog no: A11004; 1:1000. The antibodies were prepared in blocking buffer and incubated for 1 hour at RT. The nuclei were stained with 4′,6-diamidino-2-phenylindole (2 min, 25 ^{o}C). The entire procedure was carried out in a humid chamber at RT. All slides were imaged on a Zeiss confocal microscope, and analysed using the ImageJ software (version 2.1.0/1.53c)[62, 63].

Results

Purification of NΔ60-ABHD14A: Full length WT human ABHD14A contains 271 amino acids and structurally possesses two domains based on a bioinformatics analysis: a transmembrane helix (amino acids: 32 – 55) and the ABHD region (amino acids: 71 – 268). First, we attempted to express the codon optimized full length WT human ABHD14A recombinantly in *E. coli*, but were unsuccessful, despite screening various *E. coli* competent cells, in combination with changing the position of the 6X-His tag (N- or C-terminus) and temperature for inducing expression. Hence, we decided to sequentially truncate the full length protein by sequentially deleting 10 amino acids at a time from the N-terminal end of human ABHD14A, and recombinantly express these truncated variants in *E. coli*. From this experiment, we found that deleting 50 amino acids from the N-terminal end of human ABHD14A did not have any effect on either expression or solubility of the truncated protein. However, removing the entire N-terminal transmembrane helix (deleting 60 or more amino acids from the N-terminus) remarkably improved both the expression and solubility of these truncated variants of human ABHD14A. Thus, based on this initial screening, we found that deleting the first 60 amino acids from the N-terminus of human ABHD14A (NΔ60-WT

ABHD14A variant) was best suited for subsequent biochemical analysis, as it retained most of the full-length protein sequence, after removal of the N-terminal helix (Figure 3.2).

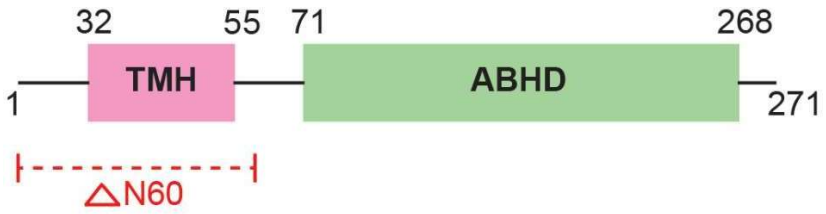

Residues deleted from N-terminus	Expression	Solubility
1 - 10	Poor	Poor
1 - 20	Poor	Poor
1 - 30	Poor	Poor
1 - 40	Poor	Poor
1 - 50	Moderate	Poor
1 - 60	Good	Good
1 - 66	Good	Good

Figure 3.2: Schematic representation of the human ABHD14A structure. Based on its protein sequence, human ABHD14A is predicted to contain a N-terminal transmembrane helix (TMH) (residues 32 – 55) and an overall a/b-hydrolase domain (ABHD) (residues 71 – 268). The table at the bottom shows the expression and solubility status of various N-terminal truncated variants of human ABHD14A recombinantly expressed in E. coli. Amongst the truncated variants, NΔ60-ABHD14A was taken forward for biochemical analysis. The terminology for poor /good expression was used based on whether we see a band for ABHD14A on a Coomassie gel on induction. Poor expression meant that no band was visible. Moderate meant that we could see it on a western blot and good expression implied that we could see a distinct band in Coomassie staining.

The possible reason for the insolubility and instability of the purified full-length (WT) ABHD14A is the presence of the 60 residues long hydrophobic region, which is partially disordered, and the rest constitutes an alpha helix. These hydrophobic regions impede the proper folding in an aqueous environment, and thus, affect solubility. Deleting these 60 amino acids resulted in the globular ABH domain of the protein, which is highly soluble, and this domain could fold

independently with independent enzymatic activity. Therefore, the deletion made the protein more soluble.

Having confirmed the expression and solubility of the NΔ60-WT ABHD14A variant, next, we purified this truncated protein using affinity chromatography to near homogeneity (> 95% purity), with a typical yield of 5 mg/L culture (Figure 3.3). The catalytic serine for human ABHD14A is Ser-171, and we generated the NΔ60-S171A ABHD14A variant using site-directed mutagenesis. We purified this mutant to near homogeneity using affinity chromatography (yield 1.5 mg/L culture) and confirmed by analytical gel-filtration that both the truncated ABHD14A variants, NΔ60-WT and NΔ60-S171, behaved alike in this experiment (Figure 3.4).

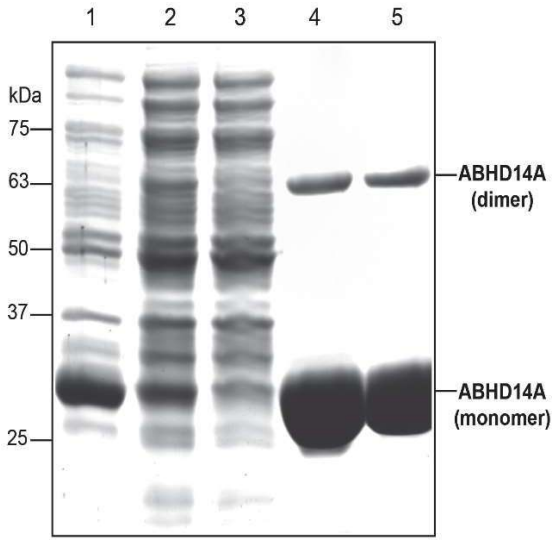

Figure 3.3: Purification of NΔ60-WT ABHD14A. A representative coomassie gel for the scheme towards purifying NΔ60-WT ABHD14A recombinantly from E. coli. The monomer and dimer bands of NΔ60-WT ABHD14A were verified for identity using in-gel proteomics analysis. 1 = Whole cell lysate; 2 = supernatant after sonication; 3 = flow through after Ni-NTA column; 4 = elute from Ni-NTA column; 5 = final protein after dialysis.

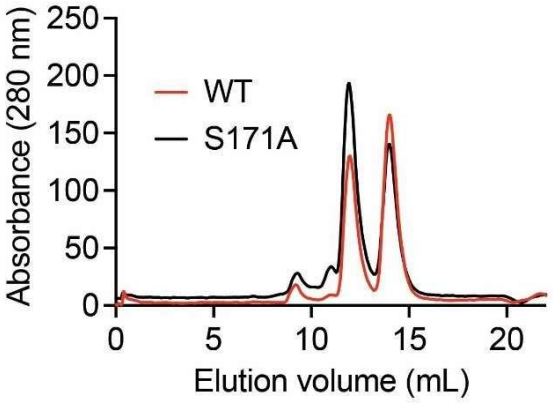

Figure 3.4. Analytical gel filtration of NΔ60-ABHD14A variants. Representative UV-traces from an analytical gel filtration experiment showing that NΔ60-WT ABHD14A and NΔ60-S171A ABHD14A have similar oligomerization states and in turn, tertiary structures.

Gel-based ABPP assays with ΔN60-ABHD14A variants: To determine activity status of the NΔ60-ABHD14A variants, we first used the established gel-based ABPP assays. Here, we found that as a function of an increasing enzyme concentration (0.2 – 10 μM), NΔ60-WT

ABHD14A, but not NΔ60-S171 ABHD14A, displayed robust dose-dependent activity against the FP-rhodamine activity probe (5 μM), which was kept constant in this assay. Along similar lines, we found that as a function of increasing the FP-rhodamine activity probe concentration (0.2 – 5 μM), and keeping the enzyme concentration constant (2 μM), NΔ60-WT ABHD14A again showed robust dose-dependent activity, while the NΔ60-S171 ABHD14A mutant showed no activity at all in this gel-based ABPP experiment (Figure 3.5). As a control, we used heat-denatured NΔ60-WT ABHD14A (10 μM) in both the gel-based ABPP experiments, and found that unfolding NΔ60-WT ABHD14A resulted in complete loss of enzymatic activity. This established an equivalence between denatured NΔ60-WT ABHD14A and the NΔ60-S171 ABHD14A mutant, and we decided to use denatured NΔ60-WT ABHD14A as a negative control for all subsequent biochemical assays.

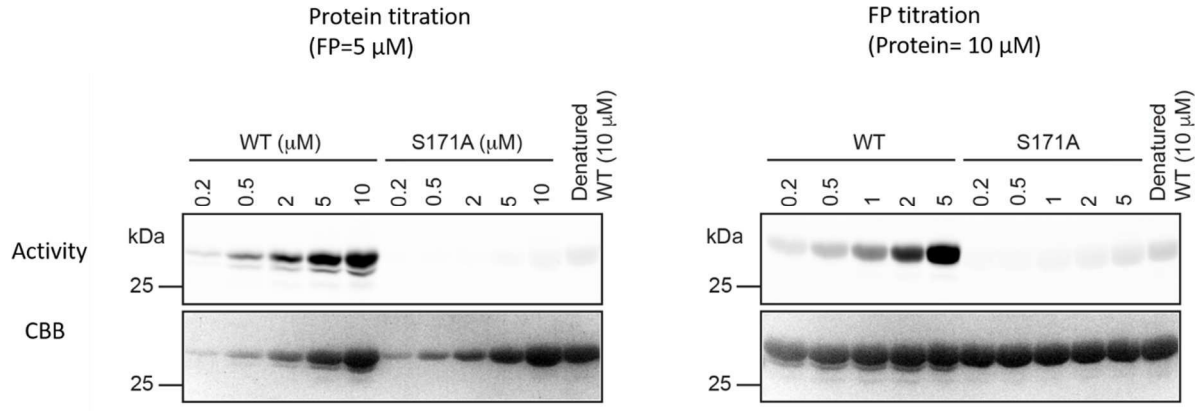

Figure 3.5:Gel-based ABPP analysis on the NΔ60-ABHD14A variants. (A, B) Gel-based ABPP assays on the WT and S171A human NΔ60-ABHD14A variants, showing robust dose-dependent activity of NΔ60-WT ABHD14A, but not NΔ60-S171A ABHD14A, as a function of increasing (A) enzyme concentration (0.5 – 10 μM) or, (B) activity probe (FP-rhodamine) concentration (0.2 – 5 μM), respectively, while keeping the other constant [FP-rhodamine (5 μM) in panel A, enzyme concentration (2 μM) in panel B]. The gel-based ABPP experiments were performed three independent times with reproducible results each time.

Acetyltransferase activity of ΔN60-WT ABHD14A: To complement the gel-based ABPP assays, we also performed substrate hydrolysis assays with p-nitrophenyl-esters using established protocols[10]. Here, we incubated native NΔ60-WT ABHD14A and its denatured form with p-nitrophenyl-acetate (pNP-acetate) (500 μM). From this qualitative assay, we found that native NΔ60-WT ABHD14A, but not its denatured form, efficiently produced *p*-nitrophenolate from pNP-acetate (approximately 5-fold better) (Figure 3.6).

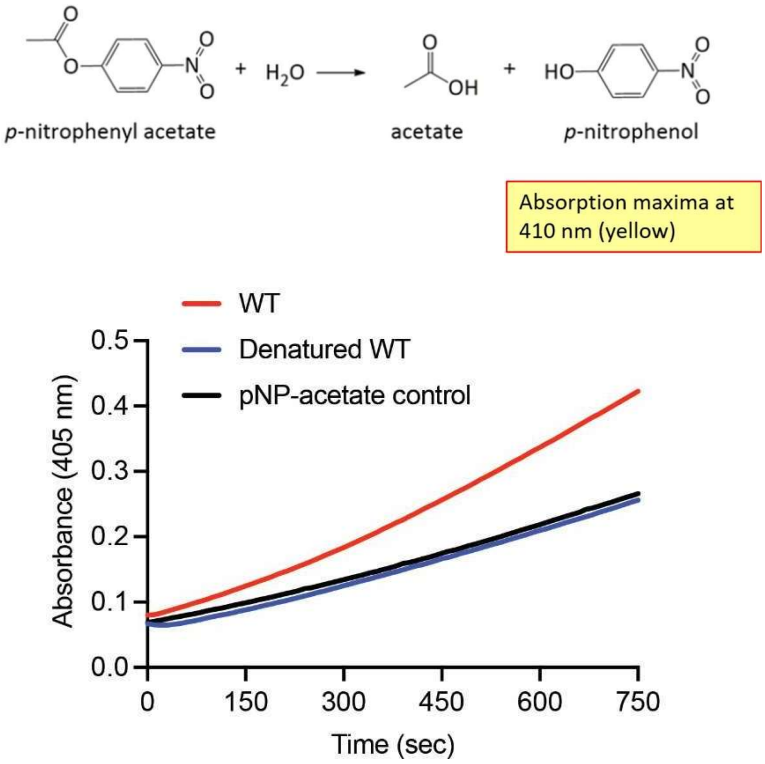

Figure 3.6: NΔ60-WT ABHD14A can hydrolyze pNP-acetate. Colorimetric enzymatic assay showing more activity of the native NΔ60-WT ABHD14A, compared to its denatured form, against pNP-acetate (500 μM). The colorimetric assays were performed three independent times with reproducible results each time.

We also tested other long acyl-chain containing p-nitrophenyl-esters (e.g. butyrate, octonoate, decanoate, dodecanoate, palmitate), and found that ΔN60-WT ABHD14A was unable to produce *p*-nitrophenolate from any of these under similar assay conditions. It has been previously shown that a closely related mammalian protein ABHD14B possesses a unique ping-pong type acetyltransferase activity with Co-A being the acetyl-group acceptor, and functions as a lysine deacetylase in mammalian cells and tissues. Given the high sequence and structural homology between the two ABHD14 proteins, we wanted to check if ΔN60-WT ABHD14A also possesses any acetyltransferase activity. To test this premise, ΔN60-WT ABHD14A (10 μM) was incubated with Co-A or acetyl-Co-A (1 mM each), and the reaction was initiated by adding pNP-acetate (50 μM). Consistent with an acetyltransferase activity, we found that Co-A, but not acetyl-Co-A, significantly increased the rate of pNP-acetate hydrolysis (Figure 3.7). Consistent with findings from experiments with human ABHD14B, this activity profile is evidence for the formation of acetyl-Co-A from pNP-acetate with Co-A

being the acetyl-group acceptor (heightened acetyl-Co-A formation in the experiment was also verified by LC-MS analysis). Overall, our studies show that ΔN60-WT ABHD14A indeed possesses
an acetyltransferase activity similar to its close mammalian homolog ABHD14B.

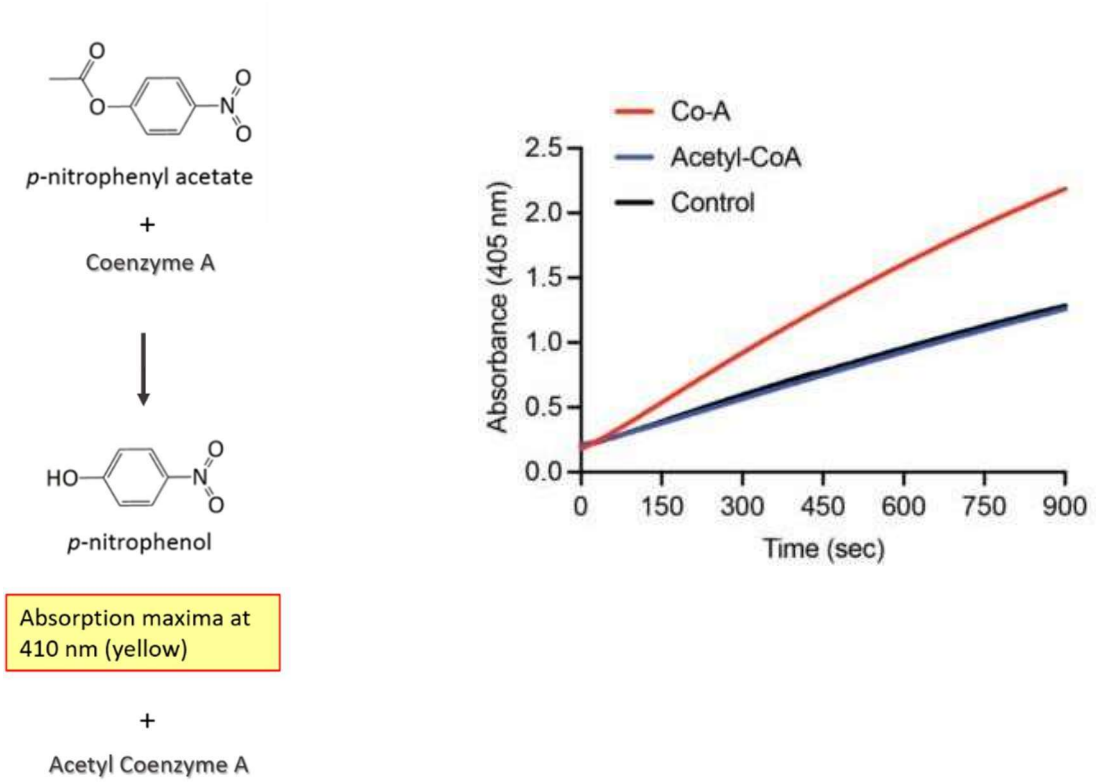

Figure 3.7: NΔ60-WT ABHD14A has acetyltransferase activity. Colorimetric enzymatic assay with pNP-acetate (500 μM), showing an increase in the rate of enzymatic reaction following incubation of NΔ60-WT ABHD14A with Co-A, but not acetyl-Co-A. This is consistent with an acetyltransferase reaction that results in the formation of acetyl-Co-A, when Co-A and pNP-acetate are incubated with NΔ60-WT ABHD14A. The colorimetric assays were performed two independent times with reproducible results each time.

Characterization of an anti-ABHD14A antibody: Since we were successful in purifying ΔN60-WT ABHD14A in good yield and high purity, we decided to generate an anti-ABHD14A antibody (polyclonal) from a single rabbit using in house protocols at the NFGFHD at IISER Pune. Post-immunization and the terminal bleed, we obtained 30 mL of serum, a fraction of which (12 mL of serum) was used to purify approximately 3.5 mg of anti-ABHD14A polyclonal antibody from one rabbit. To validate the compatibility in Western

blotting experiments, we first tested the serum (from the terminal bleed) and purified antibody against varying amounts (0.01–1 µg) of NΔ60-WT ABHD14A and NΔ60-S171A ABHD14A (Figure 3.8). From this Western blot analysis, we found that both the serum and purified polyclonal antibody at a dilution 1:1000 could reliably detect 50 ng of NΔ60-ABHD14A variants, thus, giving us confidence that this in-house generated polyclonal antibody might in fact be useful in detecting endogenous ABHD14A (if present) in immortalized mammalian cell lines and adult mouse tissues by Western blotting.

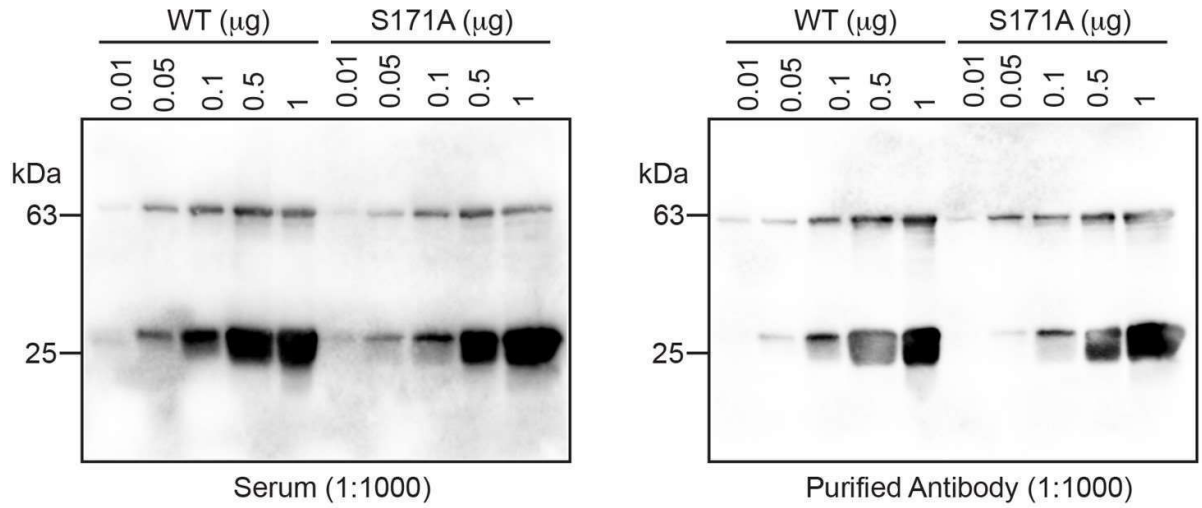

Figure 3.8. Characterization of the anti-ABHD14A antibody. Western blot analysis of a rabbit polyclonal anti-ABHD14A antibody (left panel, serum after terminal bleed at a dilution of 1:1000; right panel, purified antibody at a dilution of 1:1000) tested against varying amounts (0.01 – 1 µg) of recombinantly purified NΔ60-WT ABHD14A and DN60-S171A ABHD14A. All Western blot experiments were performed three independent times with reproducible results each time.

Several large-scale gene expression databases suggest that ABHD14A is present in various mammalian cell lines and adult mouse tissues. However, in comparison, there are very limited studies that quantify the ABHD14A protein levels in any mammalian cell lines or tissues. To investigate this, we tested our anti-ABHD14A polyclonal antibody and surprisingly found that ABHD14A was absent in all the immortalized mammalian cell lines and adult mouse tissues tested by us. To confirm that this result wasn't an artefact of our antibody, we also purchased a validated commercially available antibody and found similar results in the same Western blot analysis (Figure 3.9) done with femto ECL. To ensure that all the Western blot experiments were working well, we also used 50 ng of NΔ60-WT ABHD14A as a positive control in these immunoblotting experiments and were able to detect very good signals for this positive control in all the experiments. Taken together, this result suggests that contrary to information available from

large-scale gene expression databases, ABHD14A is perhaps physiologically produced on demand or in response to specific stimuli and/or environmental conditions in mammalian cells and tissues. We cannot hypothesize on these stressors since the exact function of ABHD14A is yet to be determined. But previous studies have hinted on transcriptional upregulation, particularly in developmental processes like germ cell migration.

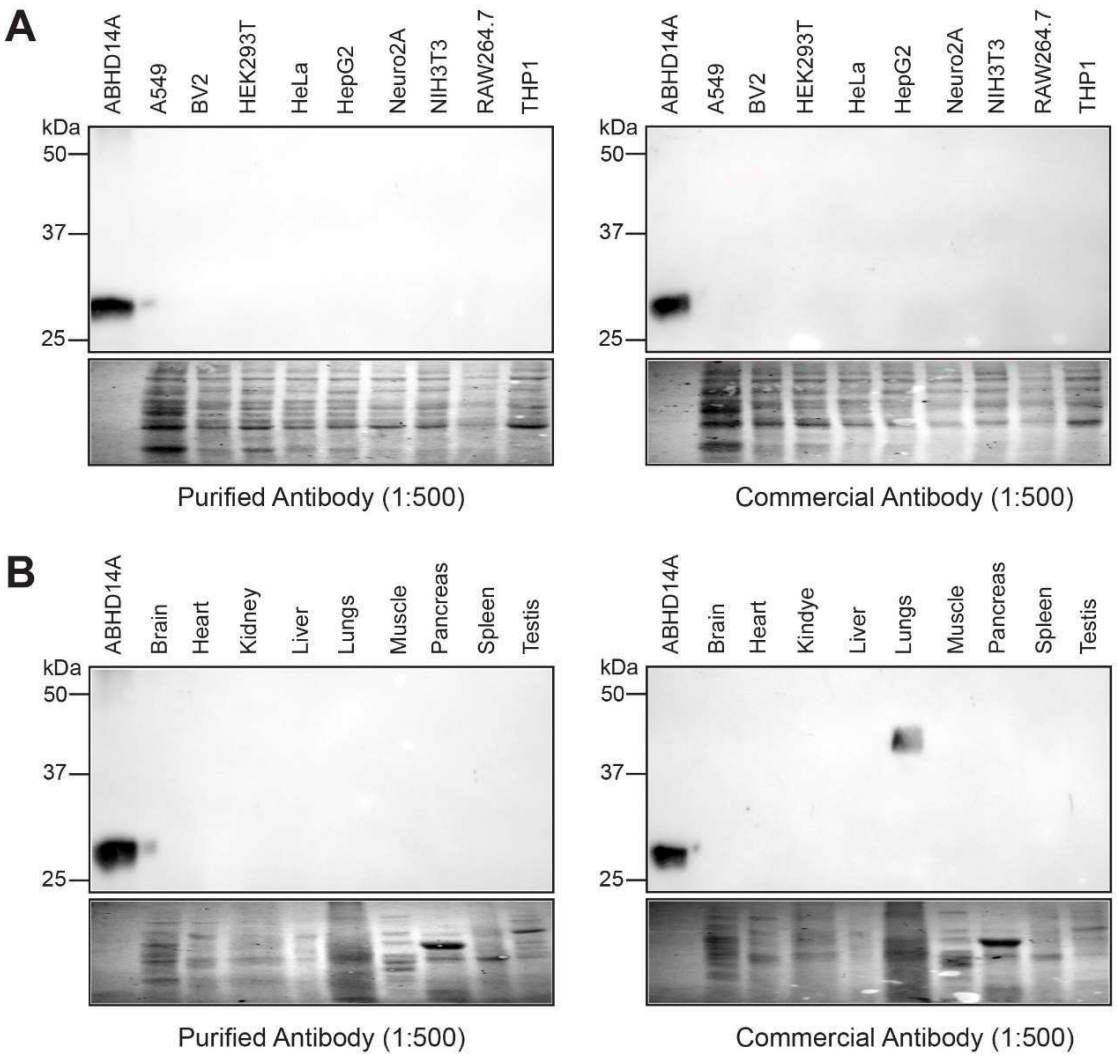

Figure 3.9. Detection of ABHD14A in mammalian cells and mouse tissues by immunoblotting. (A, B) Western blot analysis with our rabbit polyclonal anti-ABHD14A antibody and a commercially available rabbit polyclonal anti-ABHD14A antibody tested against (A) proteomes (50 µg) of different immortalized mammalian cell lines, and (B) proteomes (50 µg) of different adult mouse tissues. The Western blots show that ABHD14A is not detected (or below detection levels) in any of the immortalized cell lines or adult mouse tissues tested. The

NΔ60-WT ABHD14A (50 ng) was used as a positive control in all the immunoblotting experiments. All Western blot experiments were performed three independent times with reproducible results each time.

Expression and localization of ABHD14A in HEK293T cells: Since we were unable to find a suitable immortalized mammalian cell line to study endogenous ABHD14A, we decided to (over)express and map the subcellular localization of rat ABHD14A in the mammalian HEK293T cell line. The human and rat ABHD14A proteins have very high sequence similarity (87%) and complete conservation of residues from the N-terminal transmembrane helix and the ABHD region of the polypeptide sequence. Hence, both proteins are likely to behave the same in these experiments and therefore, we decided to use the rat ABHD14A for the experiments in HEK293T cells. Using a lipofectamine-based transient transfection strategy, we expressed WT and the catalytically inactive S142A variant of rat ABHD14A in HEK293T cells. Relative to a mock control, the overexpression of both WT and S142A variant of rat ABHD14A in the membrane lysates of HEK293T cells was confirmed by Western blot analysis using our anti-ABHD14A polyclonal antibody. Consistent with the biochemical experiments described earlier with the NΔ60-ABHD14A variants, we found that relative to the mock control, WT rat ABHD14A, but not the corresponding catalytically inactive S142 mutant, showed robust activity in the membrane lysates of HEK293T cells by gel-based ABPP analysis. This result conclusively shows that full-length mammalian ABHD14A is indeed an active enzyme, when (over)expressed in mammalian cells.

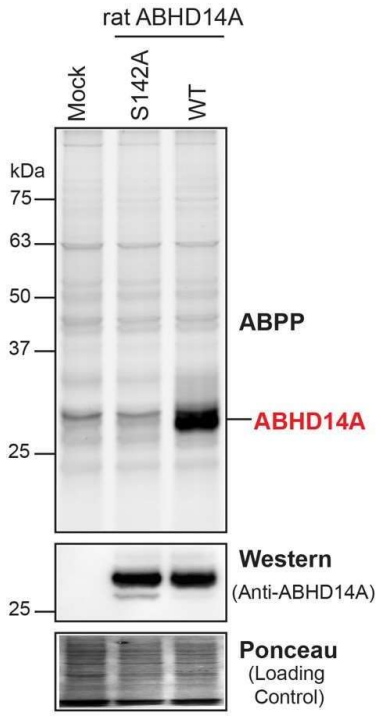

Figure 3.10: Activity of full-length rat ABHD14A in HEK293T cells. Membrane proteomes (50 µg) of HEK293T cells transfected with mock, WT rat ABHD14A, or S142A rat ABHD14A were assessed by gel-based ABPP (top panel), Western blot analysis with our anti-ABHD14A

antibody (middle panel), and Ponceau S staining (bottom panel). This experiment was done 3 times with reproducible results each time.

Full length mammalian ABHD14A possesses a conserved N-terminal transmembrane helix that presumably anchors this enzyme to the membrane of some cellular organelle. To assess the subcellular localization of ABHD14A, we performed an immunofluorescence analysis (IFA) on HEK293T cells that (over)expressed WT rat ABHD14A using our anti-ABHD14A polyclonal antibody. We found from this cellular IFA, that cellular fluorescent signal for ABHD14A (red channel) was only visible when ABHD14A was (over)expressed in HEK293T cells, and the mock control samples showed negligible signal for ABHD14A. This experiment validated that our anti-ABHD14A antibody was also compatible for cellular IFA experiments. Quite interestingly, (over)expressed ABHD14A showed a dense aggregation pattern, consistent with proteins that localize to the Golgi apparatus. Indeed, we found that the intense cellular fluorescence signal for ABHD14A (red channel) highly co-localized with the cellular fluorescence signal for a bonafide Golgi apparatus marker, GM130 (green channel). We also performed cellular immunofluorescence experiments with other organellar markers (e.g. endoplasmic reticulum, plasma membrane, mitochondria), but did not find any co-localization with ABHD14A, suggesting that ABHD14A is predominantly localized to the Golgi apparatus, when expressed in mammalian cells.

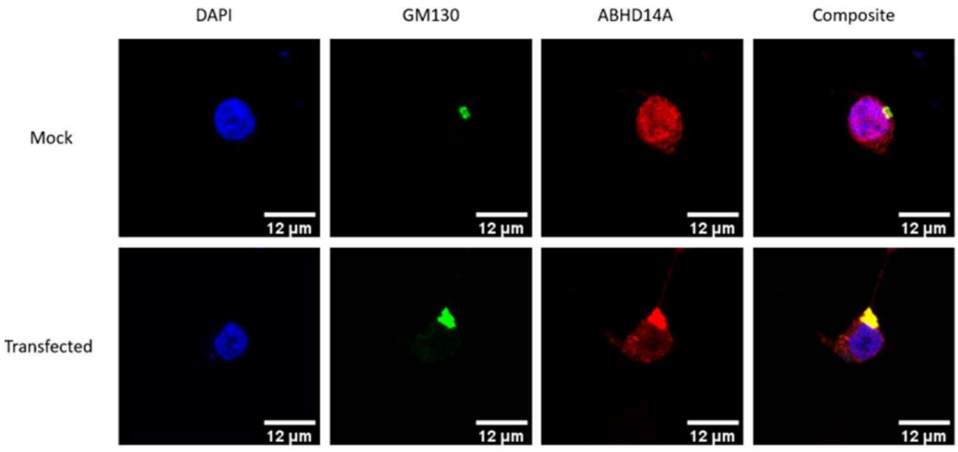

Figure 3.11: Cellular localization of (over)expressed ABHD14A in HEK293T cells. A cellular immunofluorescence analysis (IFA) in HEK293T cells shows that (over)expressed ABHD14A is present in Golgi-apparatus, and the cellular fluorescence for ABHD14A (in the red channel) is seen only when ABHD14A is (over)expressed in HEK293T cells. The cellular IFAs were performed three independent times with reproducible results each time

Discussion

Until now, ABHD14A had been known almost exclusively from sequence predictions and structural modelling, with no consensus on its catalytic activity, substrate range, or cellular localization. By integrating biochemical assays with newly developed immunological tools and a mammalian expression system, our findings enable ABHD14A to be placed more concretely within the mSH family, while simultaneously revealing surprising features that distinguish it from established members of this enzyme class.

A major understanding from this study is that ABHD14A is an active serine hydrolase with the predicted active site residues responsible for activity. It is also capable of using Coenzyme A to turnover pNP-acetate, in a ping-pong type of reaction. This is similar to the hydrolase activity of ABHD14B.

A second major insight derives from our protein-level expression analyses. While public transcriptomic and proteomic resources consistently report widespread ABHD14A expression in human tissues and cells[64-68], our experimental data challenge these predictions. Using two independent antibodies, including a rigorously validated polyclonal reagent generated in this study, we were unable to detect endogenous ABHD14A in any immortalized cell line or adult mouse tissue examined. This discrepancy highlights limitations of high-throughput resources, where detection thresholds, peptide inference issues, or reliance on mRNA abundance can lead to overestimated protein prevalence[69, 70]. The absence of protein-level detection suggests that ABHD14A expression is either extremely low under basal conditions or is tightly regulated and induced only in specific physiological contexts. Such context-dependent expression has been documented for several mSHs involved in stress responses, lipid remodeling, and immune activation, raising the possibility that ABHD14A plays a similarly specialized role that is not captured in standard culture or steady-state tissue conditions.

Our cellular experiments provide additional clues about potential physiological functions. When expressed in HEK293T cells, full length ABHD14A localizes predominantly to the Golgi apparatus, distinguishing it from many mSHs that reside in the cytosol or endoplasmic reticulum. Golgi-localized hydrolases or transferases are often involved in lipid maturation, vesicular trafficking, glycoprotein processing, or regulation of secretory pathways[71, 72]. The dense punctate signal observed for ABHD14A is characteristic of enzymes associated with Golgi membranes and suggests that its functional substrates may include proteins or metabolites trafficking through this secretory system[73, 74]. Whether ABHD14A acts

upstream (e.g., regulating acetyl-CoA pools at the Golgi), downstream (e.g., modifying lumen-facing proteins), or in parallel with canonical Golgi enzymes remains an open question. Importantly, the catalytic inactivity of the S142A mutant in both recombinant assays and cellular ABPP confirms that the endogenous activity observed in cells is intrinsic to ABHD14A and not attributable to off-target effects associated with its overexpression.

Beyond the biochemical and cellular findings, this study also provides valuable methodological tools that will enable future work. The successful expression of a soluble N-terminally truncated variant overcomes a long-standing barrier to its biochemical characterization. The newly generated high-affinity anti-ABHD14A polyclonal antibody now makes it possible to screen physiological conditions, developmental stages, or disease states in which ABHD14A expression may be induced. Together, these tools set the stage for more targeted investigations that extend well beyond what was previously feasible.

CHAPTER 4

MASS SPECTROMETRY BASED METABOLOMICS STUDIES TO IDENTIFY PUTATIVE TARGETS FOR THE METABOLIC PATHWAYS REGULATED BY ABHD14A

Cultured cells can be used as a model system to modify protein expression via transient expression or silencing of protein expression. These altered systems are a very good tool to assess perturbations in the homeostatic state based on the change in the proteome composition upon protein expression induction of knockdown. Since ABHD14A was biochemically characterised as an active serine hydrolase with a Golgi specific localisation. We wanted to evaluate the activity of the protein in a cellular context with biological substrates in endogenous systems.

We used an untargeted metabolomics approach using mass spectrometry to fish for putative substrates or conversion products for the ABHD14A protein. These metabolites could be primary and/or secondary targets for the turnover of ABHD14A enzymatic activity. The experimental paradigm used for these experiments used HEK293T cells without ABHD14A expression as primary control and cells expressing ether WT or mutant rat ABHD14A protein as test samples. Any perturbation in the levels of any species in WT expressing cells in comparison to the Mock cells would represent a possible candidate for substrate or product identification (Figure 4.1). A comprehensive list of metabolites could also give us an idea of the pathways regulated by ABHD14A activity, when clustered according to metabolic conversion pathways. We performed metabolomics experiments *in vitro* as well as *in vitro* to corroborate the data for altered species. The *in vitro* assessment gives us an advantage of using active protein in standard conditions, while the experiments with cells give us a more physiologically relevant scenario about its activity and related changes in cellular metabolites.

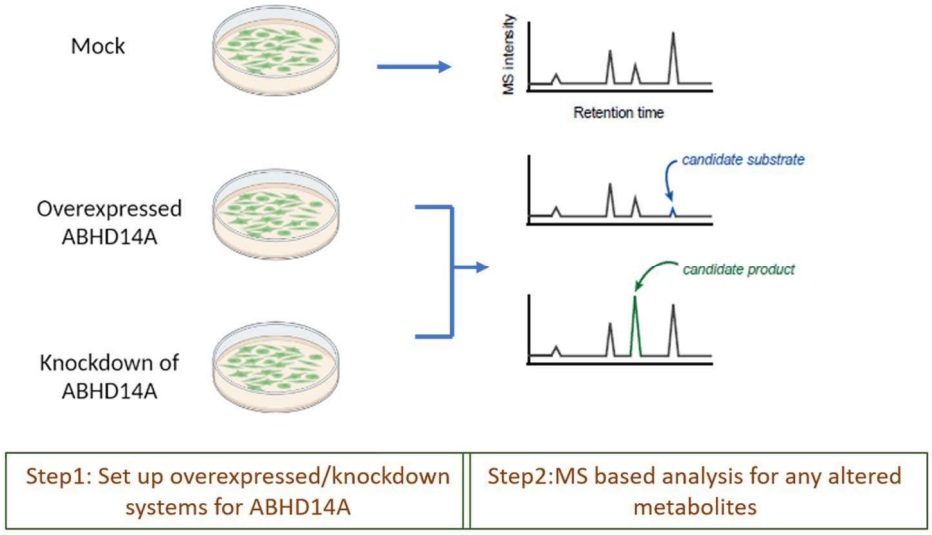

Figure 4.1: Planned experimental paradigm to identify ABHD14A substrates and products in the cell

Materials

Unless otherwise mentioned, media and consumables for mammalian cell cultures were purchased from HiMedia; chemicals, and reagents were purchased from Sigma-Aldrich; MS grade solvents were purchased from JT Baker; and chromatography columns and related accessories for LC-MS/MS analysis were purchased from Phenomenex.

Methods

ABHD14A activity assessment *in vitro:* For the *in vitro* experiments, we used HEK293T cell metabolites after extraction and treated them with 10µM concentration of either protein: denatured, mutant and WT for 1 hour at 37°C,. Following this, the metabolites were reextracted using the same procedures reported later and then analysed by LC/MS.

ABHD14A activity assessment *in vitro with cells:* HEK293T cells were transiently expressed with WT or S142A rat ABHD14A using protocols previously reported. Cells without any protein expression were reported as 'Mock' to be used as a control system. After 60 hours of protein expression induction, the cells were harvested and washed with 1XPBS, normalized with protein amount in all the three systems and then used for metabolite extraction using procedures mentioned later.

Metabolite extraction and LC-MS/MS analysis:

Non-Derivatized Polar Metabolites Extraction: Briefly, the cell pellets were resuspended in 600 µL of 75% (v/v) ethanol with respective internal standards [2 nmol of ^{13}C-glucose (Cambridge Isotopes, catalog# CLM-1396) for non-derivatized metabolites and 0.1 nmol of D4-succinic acid (Cambridge Isotopes, catalog# DLM-2307) for derivatized metabolites]. The suspension was then incubated at 80 °C for 3 min with constant shaking followed by incubation on ice for 5 min. The suspension was then centrifuged at 20,000*g* for 10 min at 4 °C. The supernatant formed contained the desired polar metabolites and was transferred to a new tube, dried under vacuum, and stored at −40/-80 °C until LC-MS/MS analysis.

Derivatized Polar Metabolites Extraction: TCA cycle intermediates are analysed better when derivatised. In order to do this, the dried extract from the final step of non-derivatised polar metabolites extraction is utilised. The dried extract was resuspended in 150 µL of water and 75 µl of 1M N-(3-dimethylaminopropyl)-N′-ethylcarbodiimide (EDC)(prepared in 13.5 mM pyridine buffer, pH 5.0) (Sigma, catalog# E7750) and mixed gently. Then, 150 µL of 0.5 M *O*-benzylhydroxylamine (Sigma, catalog# B22984) (OBHA), prepared in 13.5 mM pyridine buffer at pH 5.0, was added to the above mixture and incubated by shaking for 1 h at 25 °C. Following this, 350 µl of ethyl acetate was added to the mixture and mixed by shaking for 10 min followed by centrifugation at 3,000*g* for 5 min at 4 °C. The top layer was transferred to a new vial, and the ethyl acetate extraction repeated twice. The top layers from all three rounds of extraction were pooled together, dried under vacuum, and stored at −40/-80 °C until LC-MS/MS analysis.

Amino acids Extraction: The cell pellets were resuspended in 200 µl of 80% (v/v) methanol containing 2 nmol ^{13}C-alanine (Cambridge Isotopes, catalog# CLM-116) as an internal standard, vortexed, and incubated on ice for 10 min. The mixture was then centrifuged at 15,000*g* for 10 min at 4ºC. For every 70 µL of the supernatant, 30 µL of 1.7 mM perfluoroheptanoic acid or tridecafluoroheptanoic acid was added and mixed. The metabolites were stored at −40/-80°C until the LC-MS/MS analysis.

Lipid extraction: The cells are initially resuspended in 500µL of ice cold 1X PBS. The suspension is then sonicated at 2s on, 3s off pulses for 10 seconds at 60% amplitude. The volume of the suspension was increased by adding 500µL of ice cold 1X PBS and then the 1mLsolution was transferred to a glass vial. Further, 3mL of 2:1 Chloroform: Methanol mixture

was added to this such that the final ratio is 2:1:1 Chloroform: Methanol:PBS. The Chloroform: Methanol mixture is spiked with internal standard. Internal standards used for lipid measurements were 1 nmol heptadecenoic acid (Sigma, catalog# H8896) for negative ion mode and 50 pmol of C17:0/20:4 phosphatidylcholine (Avanti Polar Lipids, catalog# LM-1002) for positive ion mode for relative quantification of lipids. The mixture was vortexed well, followed by centrifugation at 3000rpm for 15-20 minutes leading to the formation of two discernable layers with a protein disc at the interface. The lower (organic) layer was separated into a new glass vial. 50µL of formic acid was added to the remaining solution and vortexed. An equivalent volume of organic layer separated before, of Chloroform was added to this and vortexed again. This step is important for the extraction of some neutral phospholipids and other lipids that remain in the aqueous layer. The mixture was centrifuged at 3000 rpm for 15-20 minutes and the lower layer (organic) separated and pooled with the previously extracted one. The pooled layers are dried in a stream of pure nitrogen gas and the dried lipid samples are resuspended in 1mL chloroform and transferred to a new glass vial. This step ensures that some aqueous contaminants in the extracted layers because of human error wouldn't contaminate the final lipid extract. The solution is dried in a stream of pure nitrogen gas and processed for LC/MS analysis[76].

All LC/MS runs were carried out using the Auto MSMS acquisition method on an Agilent 6545 Q-TOF mass spectrometer fitted with an Agilent 1290 Infinity II UHPLC system. The dried metabolites and lipids/fatty acids were re-solubilised in appropriate solvents. For non-derivatized metabolites, a mixture of H_2O: Acetonitrile (19:1) and 5mM Ammonium Acetate was used. The derivatised metabolised were rehydrated in 50µL of MeOH: H_2O (1:1). To resuspend the lipid extracts, 200 µL of $CHCl_3$:CH_3OH (2:1) was used. 10 µL of the resuspended samples was injected into either a Phenomenex Synergi Fusion-RP column (150mm x4.6mm, 4µm, 80Å) (catalog no. 00F-4424-E0) (for polar metabolites) or a Phenomenex Gemini C18 column (50mm x 4.6mm, 5µm, 110Å) (catalog no. 00B-4435-E0) (for lipids) fitted with a Phenomenex guard column (3.2 mm x 8.0 mm) (catalog no. KJ0-4282). The LC profiles have been annexed in the end (Appendix_Table1). Data analysis for metabolites (derivatized and non-derivatized) was performed using Agilent MassHunter Qualitative Analysis 10.0 software, and all the peaks were manually validated based on relative retention times and fragments obtained, if any. All detected species were within a mass accuracy of 15ppm and quantified by measuring the area under the curve for different

metabolites that was normalised to levels in blank (if any) and levels of respective internal standards, and then normalized to the total protein content of the respective cell pellet.

Results

Metabolite changes on treatment with purified protein: The change in metabolites was calculated by normalising the amounts in wild type and S171A ABHD14A treated samples to that of the denatured protein sample. The fold change was further calculated by normalising the new Wildtype values to that of the mutant samples. With the studies with purified protein, only two replicates were used due to the variability in the data and limitations with performing the experiment. Overall, we found that there was a lot of variability in the amounts of the diverse species analysed across samples and no significant change was observed for any of the metabolites and lipids. Comprehensively, we observed an upward regulation in the levels of glycolytic intermediates and TCA cycle intermediates. Whereas, we saw an inverse trend for amino acids and most of the Phosphatidylcholine lipids (Figure 4.2).

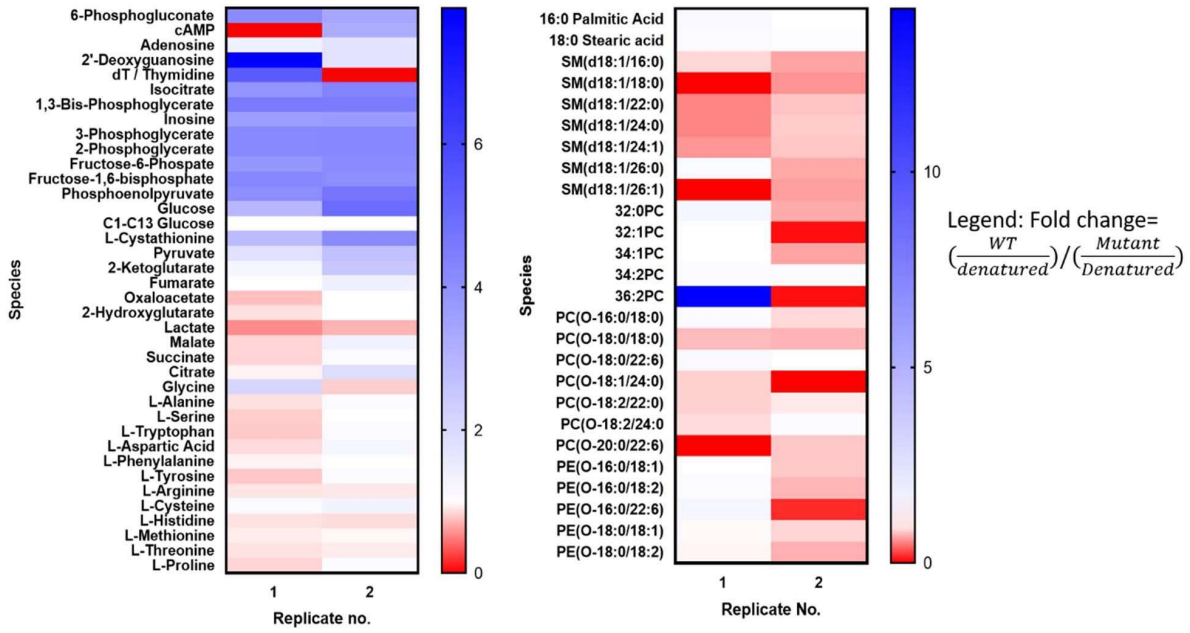

Figure 4.2: Heat map showing relative levels of metabolites treated with the Wildtype protein to that treated with the mutant protein. The levels are normalised the metabolite levels when treated with the denatured protein and to that of the levels of the internal standard for each respective metabolite class. Fold change>1 (blue) implies higher values in WT samples, Fold change=1 (white) implies no change, Fold change<1 (red) implies higher values in Mutant samples.

Metabolite changes on protein induction in HEK293T cells: Upon analysis, we found that besides Phosphatidylcholine and phosphatidylethanolamine lipids (Figure 4.3), we did not find any altered cellular levels for various glycolytic or TCA cycle intermediates, amino acids, free fatty acids (saturated, monounsaturated or polyunsaturated), other phospholipids (phosphatidic acid, phosphatidylglycerol, phosphatidylserine, and phosphatidylinositol), and other cellular metabolites in the Wildtype protein induced cells. We found significant up regulatory changes in the Wildtype sample, but milder changes were also observed for the mutant protein induced cells. This could be due to the presence of partially active protein in cells or due to cooperative binding of the protein to other binding partners that bring about these metabolic changes. These results do not align with the results from the *in vitro studies,* wherein there was a negative regulation in the levels of Phosphatidylcholine lipids on treatment with the Wildtype protein. These results can again be explained with a theory that takes into account binding partners for ABHD14A, which would stimulate pathways in the cell for the upregulation of Phosphatidylcholine species, while being absent in the *in vitro* experiments.

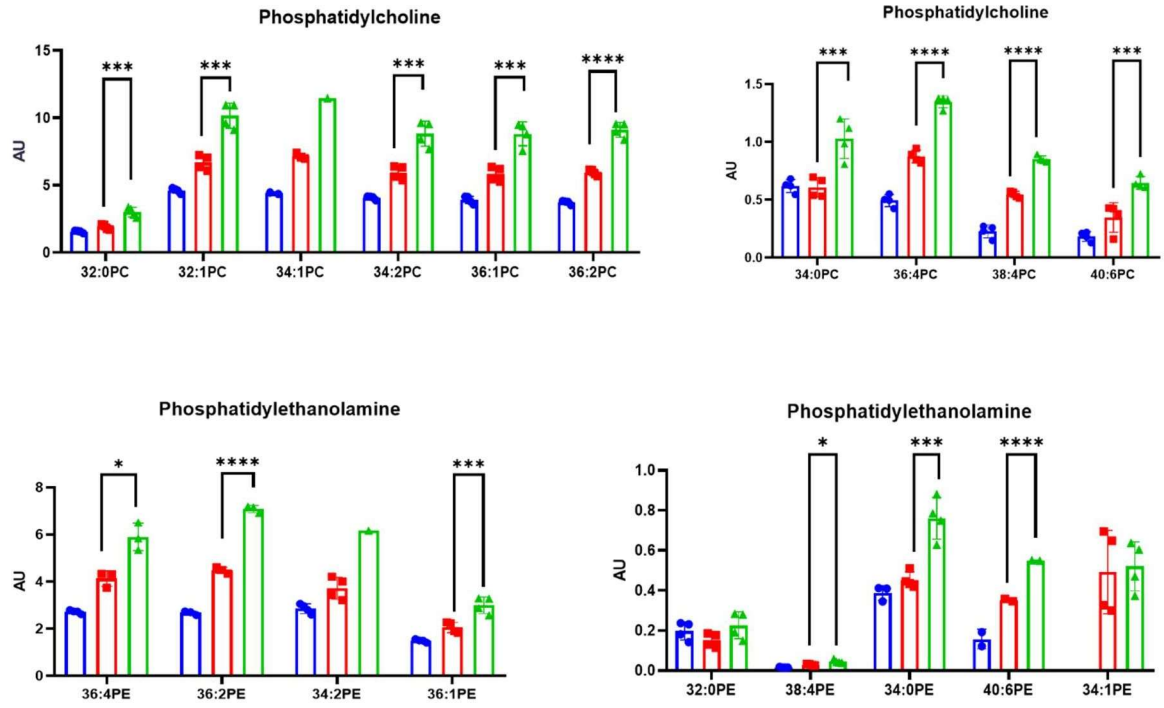

*Figure 4.3: Altered levels of Phosphatidylcholine and phosphatidylethanolamine lipids observed in HEK293T cells when induced with rat ABHD14A expression. The bar graphs show the relative levels of these lipids in the following HEK293Tcell systems: Mock /No protein (blue), S142A rat ABHD14A induced (red), Wildtype rat ABHD14A (green). Multiple t-testing was used to determine significance levels: Multiple T-Test: ***(P<0.001), ****(P<0.0001)*

Discussion

Overexpression and knockdown of proteins in cellular systems is a great tool for assessing any changes in the cells. This has been used for studying morphological as well as subcellular changes in the cell. The advent of mass spectrometry has enabled us to use these systems to quantify metabolites in the cell and therefore, assess any changes in their levels. The overexpression of an active ABHD14A in HEK293T cells did not reveal any major changes in the levels of most metabolites. Significant changes were observed for Phosphatidylcholine and Phosphatidylethanolamine species, which could be studied to recognize pathways that the protein might have roles in (either direct or regulatory). Phosphatidylcholine and Phosphatidylethanolamine lipids are majorly synthesised in the Golgi apparatus, which is where overexpressed ABHD14A is localised. This implies that there could be a possible role for the protein in the synthesis of these lipids. But these studies need to be corroborated with valid control systems and knockdown experiments to further comment on the hypothesised role.

CONCLUSIONS

This study provides the first clear biochemical and cell-based evidence that ABHD14A is an active member of the mSH family, possessing an acetyltransferase activity. We identified sequence determinants for the protein to create a repository of sequence that can be categorised as ABHD14A. We also discussed a divergent role of ABHD14A from ABHD14B over the course of evolution. By overcoming long-standing challenges in recombinant expression, we identify a soluble, catalytically competent truncated variant that enabled mechanistic studies, including the discovery of a CoA-dependent acetyltransferase activity. The generation of a robust polyclonal antibody further allowed us to probe endogenous expression, revealing that ABHD14A is absent from commonly used immortalized mammalian cell lines and adult mouse tissues despite predictions of broad transcriptional presence. Its selective Golgi localization upon heterologous expression suggests a specialized physiological role within secretory or membrane-associated pathways. We corroborated this with a metabolomic assessment of the changes in cell due to the enzymatic activity of ABHD14A. Collectively, these findings not only establish ABHD14A as an active and biochemically distinct enzyme, but also provide foundational tools and mechanistic insights that will guide future efforts to map its endogenous substrates, regulatory cues, and physiological relevance.

FUTURE DIRECTIONS

Several important directions arise from this work as we move toward determining the physiological relevance of ABHD14A. A key priority is the identification of endogenous substrates or interacting proteins, particularly in light of the enzyme's acetyltransferase activity and Golgi localization. Chemical proteomics approaches such as ABPP, CoA-reactive probe profiling, or substrate-trapping mutants will be essential for mapping the molecular environment in which ABHD14A operates. Equally important will be establishing the physiological contexts in which ABHD14A expression is induced. A previously reported study shows a transcriptomic link between ABHD14A and the transcription factor Zic1, a well-characterized regulator of early brain development[76]. The co-expression patterns of these genes in neurogenic niches coupled to population wide gene association analysis suggest that ABHD14A may participate in developmental programs that shape neuronal identity, maturation, or Golgi-dependent processing of neurodevelopmental signalling molecules, and their associations with neurological diseases[76-80].

To explore these possibilities, model systems like neural progenitor differentiation assays, mouse embryonic brain tissue, or human brain organoids could be leveraged to profile ABHD14A expression dynamics relative to Zic1 activity. It will be particularly informative to determine whether ABHD14A influences Zic1-regulated transcriptional landscapes indirectly, perhaps by modulating acetyl-CoA availability, Golgi-based processing of secreted cues, or post-translational modifications of proteins involved in neurodevelopmental signalling. High-resolution structural studies and genetic manipulation strategies, including knockout or knock-in models, will further clarify whether ABHD14A serves as a biochemical effector downstream of Zic1-regulated developmental pathways. Collectively, these future efforts promise to uncover whether ABHD14A represents a previously unrecognized enzymatic node linking mSH chemistry to the molecular architecture of brain development.

REFERENCES

1. Venter, J. C., Adams, M. D., Myers, E. W., Li, P. W., Mural, R. J., Sutton, G. G., ... & Kalush, F. (2001). The sequence of the human genome. *science*, *291*(5507), 1304-1351.
2. Rocha, J. J., Jayaram, S. A., Stevens, T. J., Muschalik, N., Shah, R. D., Emran, S., ... & Munro, S. (2023). Functional unknomics: Systematic screening of conserved genes of unknown function. *PLoS biology*, *21*(8), e3002222.
3. Long, J. Z., & Cravatt, B. F. (2011). The metabolic serine hydrolases and their functions in mammalian physiology and disease. *Chemical reviews*, *111*(10), 6022-6063.
4. Botos, I., & Wlodawer, A. (2007). The expanding diversity of serine hydrolases. *Current opinion in structural biology*, *17*(6), 683-690.
5. Bachovchin, D. A., & Cravatt, B. F. (2012). The pharmacological landscape and therapeutic potential of serine hydrolases. *Nature reviews Drug discovery*, *11*(1), 52-68.
6. Neitzel, J. J. (2010). Enzyme catalysis: the serine proteases. *Nature Education*, *3*(9), 21.
7. Hartley, B. S., & Kilby, B. A. (1954). The reaction of p-nitrophenyl esters with chymotrypsin and insulin. *Biochemical Journal*, *56*(2), 288.
8. Matthews, B. W., Sigler, P. B., Henderson, R., & Blow, D. M. (1967). Three-dimensional structure of tosyl-α-chymotrypsin. *Nature*, *214*(5089), 652-656.
9. Stroud, R. M., Kay, L. M., & Dickerson, R. E. (1974). The structure of bovine trypsin: electron density maps of the inhibited enzyme at 5 Å and at 2· 7 Å resolution. *Journal of molecular biology*, *83*(2), 185-208.
10. Bode, W., Wei, A. Z., Huber, R., Meyer, E., Travis, J., & Neumann, S. (1986). X-ray crystal structure of the complex of human leukocyte elastase (PMN elastase) and the third domain of the turkey ovomucoid inhibitor. *The EMBO journal*, *5*(10), 2453-2458.
11. Blow, D. M. (1976). Structure and mechanism of chymotrypsin. *Accounts of chemical research*, *9*(4), 145-152.
12. Blow, D. M., Birktoft, J. J., & Hartley, B. S. (1969). Role of a buried acid group in the mechanism of action of chymotrypsin. *Nature*, *221*(5178), 337-340.
13. Rajendran, A., Vaidya, K., Mendoza, J., Bridwell-Rabb, J., & Kamat, S. S. (2019). Functional annotation of ABHD14B, an orphan serine hydrolase enzyme. *Biochemistry*, *59*(2), 183-196.

14. Tupikina, E. Y., Sigalov, M. V., Alkhuder, O., & Tolstoy, P. M. (2024). Charge Relay Without Proton Transfer: Coupling of Two Short Hydrogen Bonds via Imidazole in Models of Catalytic Triad of Serine Protease Active Site. *ChemPhysChem*, *25*(12), e202300970.

15. David L, Cheah E, Cygler M, et al. The α/β hydrolase fold. *Protein Eng Des Sel*. 1992;5(3):197-211. doi:10.1093/protein/5.3.197

16. Schrag JD, Cygler M. Lipases and α/β hydrolase fold. *Methods Enzymol*. 1997;284:85-107. doi:10.1016/S0076-6879(97)84006-2

17. Nardini M, Dijkstra BW. α/β hydrolase fold enzymes: The family keeps growing. *Curr Opin Struct Biol*. 1999;9(6):732-737. doi:10.1016/S0959-440X(99)00037-8

18. Heikinheimo P, Goldman A, Jeffries C, Ollis DL. Of barn owls and bankers: A lush variety of α/β hydrolases. *Structure*. 1999;7(6). doi:10.1016/S0969-2126(99)80079-3

19. Bauer TL, Buchholz PCF, Pleiss J. The modular structure of α/β-hydrolases. *FEBS J*. 2020;287(5):1035-1053. doi:10.1111/febs.15071

20. Dimitriou PS, Denesyuk | Alexander, Takahashi S, et al. Alpha/beta-hydrolases: A unique structural motif coordinates catalytic acid residue in 40 protein fold families. *Proteins*. 2017;85:1845-1855. doi:10.1002/prot.25338

21. Denesyuk A, Dimitriou PS, Johnson MS, Nakayama T, Denessiouk K. The acid-base- nucleophile catalytic triad in ABH-fold enzymes is coordinated by a set of structural elements. *PLoS One*. 2020;15(2). doi:10.1371/journal.pone.0229376

22. Dimitriou PS, Denesyuk AI, Nakayama T, Johnson MS, Denessiouk K. Distinctive structural motifs co-ordinate the catalytic nucleophile and the residues of the oxyanion hole in the alpha/beta-hydrolase fold enzymes. *Protein Sci*. 2019;28(2):344-364. doi:10.1002/pro.3527

23. Lenfant N, Hotelier T, Velluet E, Bourne Y, Marchot P, Chatonnet A. ESTHER, the database of the α/β-hydrolase fold superfamily of proteins: Tools to explore diversity of functions. *Nucleic Acids Res*. 2013;41(D1). doi:10.1093/nar/gks1154

24. Hotelier T, Renault L, Cousin X, Negre V, Marchot P, Chatonnet A.

ESTHER, the database of the α/β-hydrolase fold superfamily of proteins. *Nucleic Acids Res*. 2004;32(DATABASE ISS.).

25. Kourist R, Jochens H, Bartsch S, et al. The α/β-hydrolase fold 3DM database (ABHDB) as a tool for protein engineering. *ChemBioChem*. 2010;11(12):1635-1643. doi:10.1002/cbic.201000213

26. Lord CC, Thomas G, Brown JM. Mammalian alpha beta hydrolase domain (ABHD) proteins: Lipid metabolizing enzymes at the interface of cell signaling and energy metabolism. *Biochim Biophys Acta - Mol Cell Biol Lipids*. 2013;1831(4):792-802. doi:10.1016/j.bbalip.2013.01.002

27. Lord CC, Thomas G, Brown JM. Mammalian alpha beta hydrolase domain (ABHD) proteins: Lipid metabolizing enzymes at the interface of cell signaling and energy metabolism. *Biochim Biophys Acta - Mol Cell Biol Lipids*. 2013;1831(4):792-802. doi:10.1016/j.bbalip.2013.01.002

28. Edgar AJ, Polak JM. Cloning and tissue distribution of three murine α/β hydrolase fold protein cDNAs. *Biochem Biophys Res Commun*. 2002;292(3):617-625. doi:10.1006/bbrc.2002.6692

29. Long JZ, Cisar JS, Milliken D, et al. Metabolomics annotates ABHD3 as a physiologic regulator of medium-chain phospholipids. *Nat Chem Biol*. 2011;7(11):763-765. doi:10.1038/nchembio.659

30. Lee HC, Simon GM, Cravatt BF. ABHD4 regulates multiple classes of N -acyl phospholipids in the mammalian central nervous system. *Biochemistry*. 2015;54(15):2539-2549. doi:10.1021/acs.biochem.5b00207

31. Poursharifi P, Madiraju SRM, Prentki M. Monoacylglycerol signalling and ABHD6 in health and disease. *Diabetes, Obes Metab*. 2017;19:76-89. doi:10.1111/dom.13008

32. Cao Y, Qiu T, Kathayat RS, et al. ABHD10 is an S-depalmitoylase affecting redox homeostasis through peroxiredoxin-5. *Nat Chem Biol*. 2019;15(12):1232-1240. doi:10.1038/s41589-019-0399-y

33. Zhuang X, Tong H, Ding Y, et al. Long noncoding RNA ABHD11-AS1 functions as a competing endogenous RNA to regulate papillary thyroid cancer progression

by miR- 199a-5p/SLC1A5 axis. *Cell Death Dis*. 2019;10(8). doi:10.1038/s41419-019-1850-4

34. Singh S, Joshi A, Kamat SS. Mapping the Neuroanatomy of ABHD16A, ABHD12, and Lysophosphatidylserines Provides New Insights into the Pathophysiology of the Human Neurological Disorder PHARC. *Biochemistry*. 2020;59(24):2299-2311. doi:10.1021/acs.biochem.0c00349

35. Xu J, Gu W, Ji K, Xu Z, Zhu H, Zheng W. Sequence analysis and structure prediction of ABHD16A and the roles of the ABHD family members in human disease. *Open Biol*. 2018;8(5). doi:10.1098/rsob.180017

36. Hoshino, J., Aruga, J., Ishiguro, A., & Mikoshiba, K. (2003). Dorz1, a novel gene expressed in differentiating cerebellar granule neurons, is down-regulated in Zic1-deficient mouse. Molecular brain research, 120(1), 57-64.
37. https://www.proteinatlas.org/ENSG00000248487-ABHD14A/tissue
38. Agarwala, S., & Ramachandra, N. B. (2021). Risk homozygous haplotype regions for autism identifies population-specific ten genes for numerous pathways. *The Egyptian Journal of Neurology, Psychiatry and Neurosurgery*, *57*(1), 1-9.
39. Cukier, H. N., Dueker, N. D., Slifer, S. H., Lee, J. M., Whitehead, P. L., Lalanne, E., ... & Pericak-Vance, M. A. (2014). Exome sequencing of extended families with autism reveals genes shared across neurodevelopmental and neuropsychiatric disorders. *Molecular autism*, *5*(1), 1-10.
40. Henrichsen, C. N., Csárdi, G., Zabot, M. T., Fusco, C., Bergmann, S., Merla, G., & Reymond, A. (2011). Using transcription modules to identify expression clusters perturbed in Williams-Beuren syndrome. *PLoS computational biology*, *7*(1), e1001054.
41. Preeprem, T., & Gibson, G. (2014). SDS, a structural disruption score for assessment of missense variant deleteriousness. *Frontiers in genetics*, *5*, 82.
42. Chang, Y. S., Tu, S. J., Chiang, H. S., Yen, J. C., Lee, Y. T., Fang, H. Y., & Chang, J. G. (2020). Genome-wide analysis of prognostic alternative splicing signature and splicing factors in lung adenocarcinoma. *Genes*, *11*(11), 1300.
43. Cava, C., Armaos, A., Lang, B., Tartaglia, G. G., & Castiglioni, I. (2022). Identification of long non-coding RNAs and RNA binding proteins in breast cancer subtypes. *Scientific Reports*, *12*(1), 1-13.

44. https://www.uniprot.org/align/

45. https://www.ebi.ac.uk/Tools/services/rest/clustalo

46. https://genome.ucsc.edu/

47. Padmanabhan, B., Kuzuhara, T., Adachi, N., and Horikoshi, M. (2004) The crystal structure of CCG1/TAF(II)250-interacting factor B (CIB), *J Biol Chem. 279*, 9615-9624.

48. Blankman JL, Long JZ, Trauger SA, Siuzdak G, Cravatt BF. ABHD12 controls brain lysophosphatidylserine pathways that are deregulated in a murine model of the neurodegenerative disease PHARC. *Proc Natl Acad Sci U S A*. 2013;110(4):1500-1505. doi:10.1073/pnas.1217121110

49. Simon, G. M., & Cravatt, B. F. (2010). Activity-based proteomics of enzyme superfamilies: serine hydrolases as a case study. *Journal of Biological Chemistry*, *285*(15), 11051-11055.

50. Rajendran, A., Soory, A., Khandelwal, N., Ratnaparkhi, G., & Kamat, S. S. (2022). A multi-omics analysis reveals that the lysine deacetylase ABHD14B influences glucose metabolism in mammals. *Journal of Biological Chemistry*, *298*(7).

51. Altschul, S. F., Madden, T. L., Schäffer, A. A., Zhang, J., Zhang, Z., Miller, W., & Lipman, D. J. (1997). Gapped BLAST and PSI-BLAST: a new generation of protein database search programs. *Nucleic acids research*, *25*(17), 3389-3402.

52. Dobson, L., Reményi, I., & Tusnády, G. E. (2015). CCTOP: a Consensus Constrained TOPology prediction web server. *Nucleic acids research*, *43*(W1), W408-W412.

53. Möller, S., Croning, M. D., & Apweiler, R. (2001). Evaluation of methods for the prediction of membrane spanning regions. *Bioinformatics*, *17*(7), 646-653.

54. Needleman, S. B., & Wunsch, C. D. (1970). A general method applicable to the search for similarities in the amino acid sequence of two proteins. *Journal of molecular biology*, *48*(3), 443-453.

55. Katoh, K., Misawa, K., Kuma, K. I., & Miyata, T. (2002). MAFFT: a novel method for rapid multiple sequence alignment based on fast Fourier transform. *Nucleic acids research*, *30*(14), 3059-3066.

56. Kumar, S., Stecher, G., Li, M., Knyaz, C., & Tamura, K. (2018). MEGA X: molecular evolutionary genetics analysis across computing platforms. *Molecular biology and evolution*, *35*(6), 1547-1549.

57. Letunic, I., & Bork, P. (2007). Interactive Tree Of Life (iTOL): an online tool for phylogenetic tree display and annotation. *Bioinformatics*, *23*(1), 127-128.

58. Varadi, M., Anyango, S., Deshpande, M., Nair, S., Natassia, C., Yordanova, G., ... & Velankar, S. (2022). AlphaFold Protein Structure Database: massively expanding the structural coverage of protein-sequence space with high-accuracy models. *Nucleic acids research*, *50*(D1), D439-D444.

59. Jumper, J., Evans, R., Pritzel, A., Green, T., Figurnov, M., Ronneberger, O., ... & Hassabis, D. (2021). Highly accurate protein structure prediction with AlphaFold. *nature*, *596*(7873), 583-589.

60. Galmozzi, A., Dominguez, E., Cravatt, B. F., & Saez, E. (2014). Application of activity-based protein profiling to study enzyme function in adipocytes. In *Methods in enzymology* (Vol. 538, pp. 151-169). Academic Press.

61. Gupta, N., Rathi, P., & Gupta, R. (2002). Simplified para-nitrophenyl palmitate assay for lipases and esterases. *Analytical biochemistry*, *311*(1), 98-99.

62. C. T. Rueden, J. Schindelin, M. C. Hiner, B. E. DeZonia, A. E. Walter, E. T. Arena and K. W.
Eliceiri, BMC Bioinformatics, 2017, 18, 529.

63. J. Schindelin, C. T. Rueden, M. C. Hiner and K. W. Eliceiri, Mol Reprod Dev, 2015, 82, 518–529.

64. M. Uhlen, L. Fagerberg, B. M. Hallstrom, C. Lindskog, P. Oksvold, A. Mardinoglu, A. Sivertsson, C. Kampf, E. Sjostedt, A. Asplund, I. Olsson, K. Edlund, E. Lundberg, S. Navani, C. A. Szigyarto, J. Odeberg, D. Djureinovic, J. O. Takanen, S. Hober, T. Alm, P. H. Edqvist, H. Berling, H. Tegel, J. Mulder, J. Rockberg, P. Nilsson, J. M. Schwenk, M. Hamsten, K. von Feilitzen, M. Forsberg, L. Persson, F. Johansson, M. Zwahlen, G. von Heijne, J. Nielsen and F. Ponten,

Science, 2015, 347, 1260419.

65. P. J. Thul, L. Akesson, M. Wiking, D. Mahdessian, A. Geladaki, H. Ait Blal, T. Alm, A. Asplund, L. Bjork, L. M. Breckels, A. Backstrom, F. Danielsson, L. Fagerberg, J. Fall, L. Gatto, C. Gnann, S. Hober, M. Hjelmare, F. Johansson, S. Lee, C. Lindskog, J. Mulder, C. M. Mulvey, P. Nilsson, P. Oksvold, J. Rockberg, R. Schutten, J. M. Schwenk, A. Sivertsson, E. Sjostedt, M. Skogs, C. Stadler, D. P. Sullivan, H. Tegel, C. Winsnes, C. Zhang, M. Zwahlen, A. Mardinoglu, F. Ponten, K. von Feilitzen, K. S. Lilley, M. Uhlen and E. Lundberg, Science, 2017, 356.
66. F. Desiere, E. W. Deutsch, N. L. King, A. I. Nesvizhskii, P. Mallick, J. Eng, S. Chen, J. Eddes, S. N. Loevenich and R. Aebersold, Nucleic Acids Res, 2006, 34, D655–658.
67. C. Wu, X. Jin, G. Tsueng, C. Afrasiabi and A. I. Su, Nucleic Acids Res, 2016, 44, D313–316.
68. C. Wu, C. Orozco, J. Boyer, M. Leglise, J. Goodale, S. Batalov, C. L. Hodge, J. Haase, J. Janes, J. W. Huss, 3rd and A. I. Su, Genome Biol, 2009, 10, R130.
69. S. H. Payne, Trends Biochem Sci, 2015, 40, 1–3.
70. T. Maier, M. Guell and L. Serrano, FEBS Lett, 2009, 583, 3966–3973.
71. B. Short and F. A. Barr, Curr Biol, 2000, 10, R583–585.
72. P. Kulkarni-Gosavi, C. Makhoul and P. A. Gleeson, FEBS Lett, 2019, 593, 2289–2305. 26. S. Munro, Trends Cell Biol, 1998, 8, 11–15. 27. B. S. Glick and V. Malhotra, Cell, 1998, 95, 883–889.
73. S. Munro, Trends Cell Biol, 1998, 8, 11–15.
74. B. S. Glick and V. Malhotra, Cell, 1998, 95, 883–889.
75. J. Hoshino, J. Aruga, A. Ishiguro and K. Mikoshiba, Brain Res Mol Brain Res, 2003, 120, 57 64.
76. Abhyankar, V., Kaduskar, B., Kamat, S. S., Deobagkar, D., & Ratnaparkhi, G. S. (2018). Drosophila DNA/RNA methyltransferase contributes to robust host defense in aging animals by regulating sphingolipid metabolism. *Journal of Experimental Biology*, *221*(22), jeb187989.S. Tang, W. Luo, C. Cheng, L. Shen, X. Wu and X. Xiao, Biochem Biophys Rep, 2025, 43, 102089.
77. A. Bouzid, M. Belcadhi, A. Souissi, M. Chelly, F. Frikha, H. Gargouri, C. Bonnet, F. Jebali, S. Loukil, C. Petit, S. Masmoudi, R. Hamoudi and M. Ben Said, Sci Rep, 2025, 15, 367.

78. J. P. Casey, T. Magalhaes, J. M. Conroy, R. Regan, N. Shah, R. Anney, D. C. Shields, B. S. Abrahams, J. Almeida, E. Bacchelli, A. J. Bailey, G. Baird, A. Battaglia, T. Berney, N. Bolshakova, P. F. Bolton, T. Bourgeron, S. Brennan, P. Cali, C. Correia, C. Corsello, M. Coutanche, G. Dawson, M. de Jonge, R. Delorme, E. Duketis, F. Duque, A. Estes, P. Farrar, B. A. Fernandez, S. E. Folstein, S. Foley, E. Fombonne, C. M. Freitag, J. Gilbert, C. Gillberg, J. T. Glessner, J. Green, S. J. Guter, H. Hakonarson, R. Holt, G. Hughes, V. Hus, R. Igliozzi, C. Kim, S. M. Klauck, A. Kolevzon, J. A. Lamb, M. Leboyer, A. Le Couteur, B. L. Leventhal, C. Lord, S. C. Lund, E. Maestrini, C. Mantoulan, C. R. Marshall, H. McConachie, C. J. McDougle, J. McGrath, W. M. McMahon, A. Merikangas, J. Miller, F. Minopoli, G. K. Mirza, J. Munson, S. F. Nelson, G. Nygren, G. Oliveira, A. T. Pagnamenta, K. Papanikolaou, J. R. Parr, B. Parrini, A. Pickles, D. Pinto, J. Piven, D. J. Posey, A. Poustka, F. Poustka, J. Ragoussis, B. Roge, M. L. Rutter, A. F. Sequeira, L. Soorya, I. Sousa, N. Sykes, V. Stoppioni, R. Tancredi, M. Tauber, A. P. Thompson, S. Thomson, J. Tsiantis, H. Van Engeland, J. B. Vincent, F. Volkmar, J. A. Vorstman, S. Wallace, K. Wang, T. H. Wassink, K. White, K. Wing, K. Wittemeyer, B. L. Yaspan, L. Zwaigenbaum, C. Betancur, J. D. Buxbaum, R. M. Cantor, E. H. Cook, H. Coon, M. L. Cuccaro, D. H. Geschwind, J. L. Haines, J. Hallmayer, A. P. Monaco, J. I. Nurnberger, Jr., M. A. Pericak-Vance, G. D. Schellenberg, S. W. Scherer, J. S. Sutcliffe, P. Szatmari, V. J. Vieland, E. M. Wijsman, A. Green, M. Gill, L. Gallagher, A. Vicente and S. Ennis, Hum Genet, 2012, 131, 565–579.

79. J. Yang, L. Bernard, J. Chen, V. K. Sullivan, J. A. Deal, H. Kim, B. Yu, L. M. Steffen and C. M. Rebholz, J Nutr, 2025, 155, 1710–1721.

APPENDIX

	Polar metabolites				Non-polar metabolites									
	Non-derivatized polar metabolites	Derivatized polar metabolites	Amino acids		Positive mode				Negative mode					
					TAG	Cholesterol	PL	Lyso-PL	FFA			PL		Lyso-PL
Solvent A	5 mM ammonium acetate in H_2O	99.9% H_2O + 0.1% FA	1 mM TDFHA in H_2O		95:5 (v/v) H_2O/MeOH + 0.1% FA + 10 mM ammonium formate				95:5 (v/v) H_2O/MeOH + 0.1% (v/v) ammonium hydroxide					
Solvent B	100% ACN	99.9% MeOH + 0.1% FA	100% ACN		60:35:5 (v/v) IPA/MeOH/H_2O + 0.1% (v/v) FA + 10 mM ammonium formate				60:35:5 (v/v) IPA/MeOH/H_2O + 0.1% (v/v) ammonium hydroxide					
Autosampler temperature	8 °C	8 °C	10		10			10	10			10		
Column oven temperature	25 °C	40 °C	30		40			30	30			30		
Flow rate	0.4 mL/min		0.2 mL/min		0.5 mL/min			0.3 mL/min	0.3 mL/min			0.3 mL/min		
Gradient	%B	Time (min)	%B	Time (min)	%B	Time (min)	%B	Time (min)	%B	Time (min)	%B	%B	Time (min)	Time (min)
	0	0	0.1	0	0	0	0	0	0	0	0	0	0	0
	5	3	0.1	2	0	4	0	5	0	4	0	0	5	5
	60	10	15	3	100	9	100	20	100	9	100	100	20	20
	95	11	15	8	100	12	100	25	100	12	100	100	25	25
	95	14	25	11	0	12.1	0	25.1	0	12.1	0	0	25.1	25.1
	5	15	25	18	0	20	0	30	0	20	0	0	30	30
	0	16	0	30										
	0	21												

Table 1: LC profile used for MS runs for metabolomics experiments.

PUBLICATIONS

1. Gupta, S., Kamat, S. S. (2025) Biochemical characterization of ABHD14A, an outlying member of the metabolic serine hydrolase family. BioRxiv: https://doi.org/10.1101/2025.11.28.691245
2. Vaidya, K., Rodrigues, G., Gupta, S., Devarajan, A., Yeolekar, M., Madhusudhan, M. S.,Kamat, S. S. (2025) Identification of sequence determinants for the ABHD14 enzymes, Proteins: Structure, Function and Bioinformatics 93 (1), 255-266.

COPYRIGHT LICENCE PERMISSION

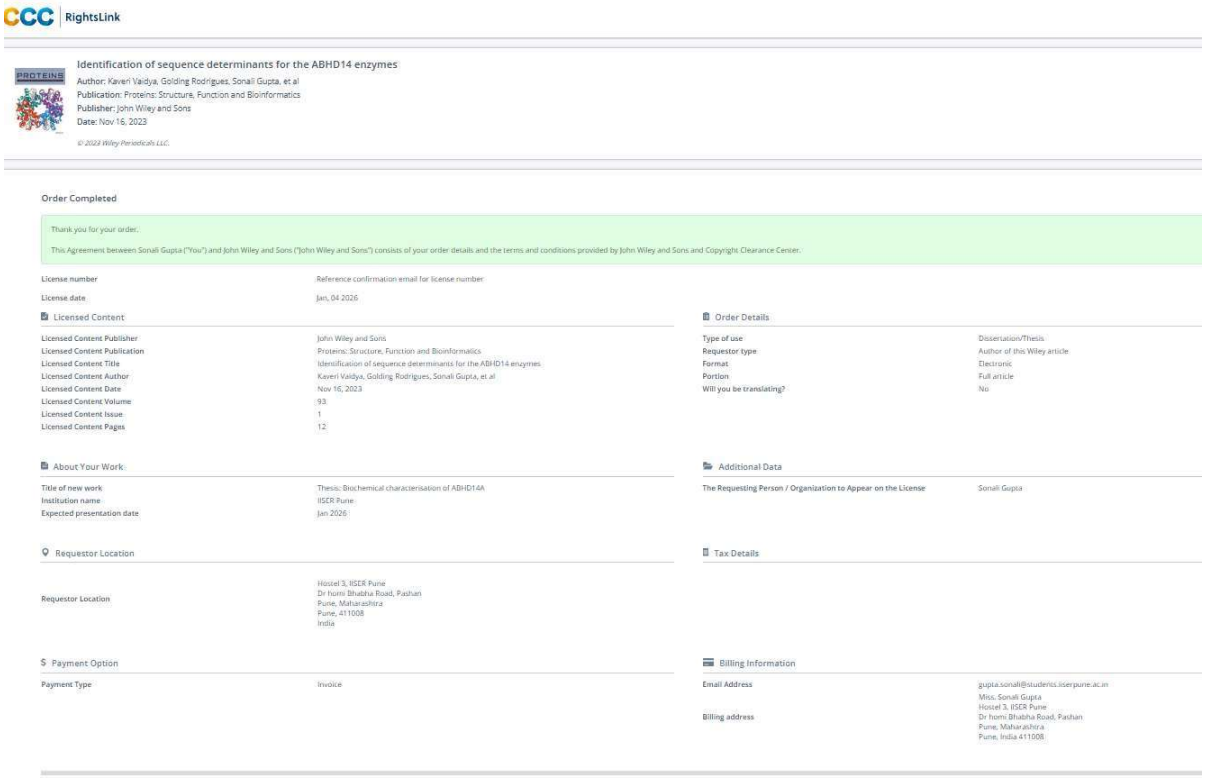

CCC | RightsLink

Identification of sequence determinants for the ABHD14 enzymes

Author: Kaveri Vaidya, Golding Rodrigues, Sonali Gupta, et al
Publication: Proteins: Structure, Function and Bioinformatics
Publisher: John Wiley and Sons
Date: Nov 16, 2023

Order Completed

Thank you for your order.

This Agreement between Sonali Gupta ("You") and John Wiley and Sons ("John Wiley and Sons") consists of your order details and the terms and conditions provided by John Wiley and Sons and Copyright Clearance Center.

License number	Reference confirmation email for license number
License date	Jan, 04 2026

Licensed Content

Licensed Content Publisher	John Wiley and Sons
Licensed Content Publication	Proteins: Structure, Function and Bioinformatics
Licensed Content Title	Identification of sequence determinants for the ABHD14 enzymes
Licensed Content Author	Kaveri Vaidya, Golding Rodrigues, Sonali Gupta, et al
Licensed Content Date	Nov 16, 2023
Licensed Content Volume	93
Licensed Content Issue	1
Licensed Content Pages	12

Order Details

Type of use	Dissertation/Thesis
Requestor type	Author of this Wiley article
Format	Electronic
Portion	Full article
Will you be translating?	No

About Your Work

Title of new work	Thesis: Biochemical characterisation of ABHD14A
Institution name	IISER Pune
Expected presentation date	Jan 2026

Additional Data

The Requesting Person / Organization to Appear on the License	Sonali Gupta

Requestor Location

Requestor Location	Hostel 3, IISER Pune Dr homi Bhabha Road, Pashan Pune, Maharashtra Pune, 411008 India

Tax Details

Payment Option

Payment Type	Invoice

Billing Information

Email Address	gupta.sonali@students.iiserpune.ac.in
Billing address	Miss. Sonali Gupta Hostel 3, IISER Pune Dr homi Bhabha Road, Pashan Pune, Maharashtra Pune, India 411008

VITA

Name: Sonali Gupta

Address: Department of Biology

IISER Pune, Dr. Homi Bhabha road

Ward no. 8, NCL colony

Pune, Maharashtra 411008

Email address: gupta.sonali@students.iiserpune.ac.in

Education: Bachelor of Science (Hons.) Biochemistry,

Daulat Ram College, University of Delhi, 2019

Master of Science, Biology, IISER Pune 2021